

AD _____

Award Number: DAMD17-01-1-0327

TITLE: Characterization of Breast Masses Using a new Method of Ultrasound
Contract Agent Imaging in 3D Mapping of Vascular Anomalies

PRINCIPAL INVESTIGATOR: Gerald L LeCarpentier, Ph.D.

CONTRACTING ORGANIZATION: University of Michigan
Ann Arbor MI 48109-1274

REPORT DATE: October 2006

TYPE OF REPORT: Final

PREPARED FOR: U.S. Army Medical Research and Materiel Command
Fort Detrick, Maryland 21702-5012

DISTRIBUTION STATEMENT: Approved for Public Release;
Distribution Unlimited

The views, opinions and/or findings contained in this report are those of the author(s) and should not be construed as an official Department of the Army position, policy or decision unless so designated by other documentation.

REPORT DOCUMENTATION PAGE				Form Approved OMB No. 0704-0188	
Public reporting burden for this collection of information is estimated to average 1 hour per response, including the time for reviewing instructions, searching existing data sources, gathering and maintaining the data needed, and completing and reviewing this collection of information. Send comments regarding this burden estimate or any other aspect of this collection of information, including suggestions for reducing this burden to Department of Defense, Washington Headquarters Services, Directorate for Information Operations and Reports (0704-0188), 1215 Jefferson Davis Highway, Suite 1204, Arlington, VA 22202-4302. Respondents should be aware that notwithstanding any other provision of law, no person shall be subject to any penalty for failing to comply with a collection of information if it does not display a currently valid OMB control number. PLEASE DO NOT RETURN YOUR FORM TO THE ABOVE ADDRESS.					
1. REPORT DATE (DD-MM-YYYY) 01-10-2006		2. REPORT TYPE Final		3. DATES COVERED (From - To) 24 Sep 01 - 23 Sep 06	
4. TITLE AND SUBTITLE Characterization of Breast Masses Using a new Method of Ultrasound Contract Agent Imaging in 3D Mapping of Vascular Anomalies				5a. CONTRACT NUMBER	
				5b. GRANT NUMBER DAMD17-01-1-0327	
				5c. PROGRAM ELEMENT NUMBER	
6. AUTHOR(S) Gerald L LeCarpentier, Ph.D. E-Mail: gllec@umich.edu				5d. PROJECT NUMBER	
				5e. TASK NUMBER	
				5f. WORK UNIT NUMBER	
7. PERFORMING ORGANIZATION NAME(S) AND ADDRESS(ES) University of Michigan Ann Arbor MI 48109-1274				8. PERFORMING ORGANIZATION REPORT NUMBER	
9. SPONSORING / MONITORING AGENCY NAME(S) AND ADDRESS(ES) U.S. Army Medical Research and Materiel Command Fort Detrick, Maryland 21702-5012				10. SPONSOR/MONITOR'S ACRONYM(S)	
				11. SPONSOR/MONITOR'S REPORT NUMBER(S)	
12. DISTRIBUTION / AVAILABILITY STATEMENT Approved for Public Release; Distribution Unlimited					
13. SUPPLEMENTARY NOTES					
14. ABSTRACT Doppler ultrasound and other imaging modalities have been used to assess characteristics of vasculature associated with malignant breast masses. 3D contrast refill imaging should help visualize slow-flow in small neo-vasculature associated with these masses. The dual-transducer method investigated is expected to provide vascular mapping while minimizing acquisition time, the major limitation of techniques such as interval-imaging (I-I) and real-time (RT) imaging. Phantom tube-flow studies confirmed the method as viable in a simple sense. Further experiments with an in vitro fixed porcine kidney provided the bulk of the data post Y2. Image volumes reconstructed using the dual-transducer method displayed remarkable spatial detail. A parametric method of visualizing mean transit times (MTTs) throughout a volume was developed, and a secondary scheme for extending the technique into clinical trials was developed. Simple MTT estimates were extended into actual perfusion estimates, using large vessel reference signals within each image plane. These signals were characterized and quantified by way of a variety of means presented in this report. There was significant consistency among methods. Results over the course of the study have been promising, and clinical trials are expected in the near future.					
15. SUBJECT TERMS None provided.					
16. SECURITY CLASSIFICATION OF:			17. LIMITATION OF ABSTRACT	18. NUMBER OF PAGES	19a. NAME OF RESPONSIBLE PERSON
a. REPORT	b. ABSTRACT	c. THIS PAGE			USAMRMC
U	U	U	UU	64	19b. TELEPHONE NUMBER (include area code)

Table of Contents

Cover.....

SF 298.....

Table of Contents

Introduction..... 1

Body 2

Key Research Accomplishments 11

Reportable Outcomes 12

Personnel 13

Conclusions 14

References 14

Appendix 16

Introduction

As mentioned in previous reports and the original proposal, the overall objective of this project has been to develop a 3D ultrasound contrast imaging system for characterizing suspicious breast masses. This report summarizes the progress made in this regard over the original grant period and no-cost extension periods. As such, with the notable exception of the summary of the final work period, much of the text is adapted and integrated from previous reports and/or refers to published or submitted work in the appendix. Appendix materials include reprints of 6 abstracts as well as two peer-reviewed papers submitted to *Ultrasound in Medicine and Biology*: (1) "Rapid 3D Imaging of Contrast Flow: Demonstration of a Dual Beam Technique" and (2) "Rapid 3D Imaging of Contrast Flow II: Application to Perfused Kidney Vasculature," in press and under revision, respectively.

The originally proposed method uses a dual-transducer scheme to map mean blood transit time in three dimensions. The method requires a fraction of the time necessary to obtain similar information using other standard contrast imaging techniques, and it should provide information related to normal and anomalous vascular characteristics in and around suspicious masses. In addition, the technique should allow visualization of areas of slow flow and microvasculature, which cannot be detected with conventional Doppler imaging methods. It is hypothesized that these measures will enhance our ability to discriminate benign from malignant lesions as well as serve to increase our understanding of tumor biology in terms of vessel formation.

The originally proposed schedule would have concluded at the end of year three; however, we eventually opted to continue method refinements and analysis techniques during two no-cost extension periods rather than entering into clinical trials with uncertainties remaining in the actual methodology. In particular, it became apparent that simple mean transit time measurements are insufficient to describe vascularity and flow characteristics. Perfusion is the quantity of interest, and its estimation requires an estimate of fractional blood volume. Our methods were investigated to this end and are presented in the body of the report.

We have not abandoned a clinical trial aspect to the work, but it has unfortunately fallen beyond the scope of the grant period. We have made significant preparations in this regard, including ongoing consultation and collaboration with GE Global Research, the latter formal arrangement funded through other sources. In addition, a modified version of the dual-transducer scanning apparatus is in place, and a scheme has been developed for a single-transducer, "dual-sweep" version of the original technique.

Body

Background:

Given that the following background text provides information regarding the impetus of the proposed work, it is essentially unchanged from our previous reports. As mentioned in the original proposal and other yearly reports, previous studies by other investigators have demonstrated characteristics of vasculature associated with malignant breast masses. These have included thin-walled blood vessels, increased microvessel density, disordered neo-vascularization penetrating the mass, arteriovenous shunting, and a variety of characteristic Doppler ultrasound and histologic findings [Lee et al. 1996, Peters-Engl et al. 1998]. Some studies strongly suggest that flow velocity demonstrates significant correlation with tumor size [Peters-Engl et al. 1998] and that parameters such as vessel count and flow velocity display significant differences between malignant and benign lesions [Madjar et al. 1994]. A shortcoming of most of these trials has been the limitation of 2D images in assessing overall vascular morphology, density, and velocity distributions.

Given the limitation of 2D studies and the relative sparseness of breast vasculature, our group has investigated the utility of 3D breast imaging for several years. Recently published results [LeCarpentier et al. 1999] indicate that one of our Doppler vascularity measures, Speed Weighted pixel Density (SWD), is statistically different for benign versus malignant lesions and comparable to ultrasound grayscale (GS) evaluation. More recent work in a 38 patient pool suggests that multi-variable indices (which include both SWD and GS features) demonstrate good results in differentiating benign from malignant breast masses well beyond GS evaluation alone [Bhatti et al. 2000]. In a follow-up study (submitted and accepted for publication), the results of the initial 38 patients (18 benign, 20 malignant) were used to form a learning set (A), and multivariable indices were established using Bayesian discriminators. In Group A, 94% specificity was achieved for the SWD-Age-GS index at 100% sensitivity. Applying the same linear function to the second pool (B) resulted in 86% specificity at sensitivity of 100% [LeCarpentier et al. 2002]. The diagnostic performance of SWD in our second patient population strongly suggests the utility of vascular indices in the characterization of breast masses.

In addition to Doppler imaging, a number of investigators have performed extensive evaluation of ultrasound contrast agents in the evaluation of blood flow. Success of low-frame-rate imaging (termed "transient response imaging" or "interval imaging") is related to the "refill" of agent into tissue [Porter and Xie 1995, Porter et al. 1997]. Monitoring refilling has estimated the perfusion in tissue [Wei et al. 1998] and specific pulsing sequences such as "Flash Echo Imaging" (Toshiba Medical Systems) and "Power Pulse Inversion" (ATL/Phillips) have been

developed on ultrasound scanners to obtain refill information. Studies at our institution [Fowlkes et al. 1998] have shown that it is possible to destroy contrast agent flow in arteries to produce interruptions with signal separation up to 30 dB. Similar interruptions allow downstream contrast agent to clear and the release of a short bolus by temporarily turning off the field [Rhee et al. 1998]. All of these methods rely on controlled destruction of contrast

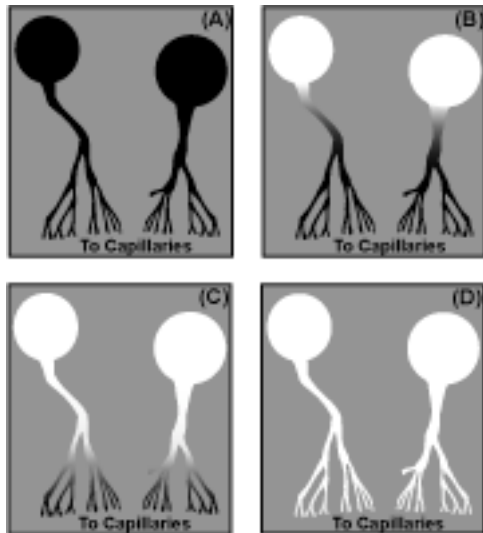


Figure1. Schematic representation of ultrasound contrast refill. An ultrasound beam is used to destroy contrast agent in all vessels in the imaging plane (A). The larger vessels quickly refill (B) and feed the smaller arteries and arterioles with fresh contrast (C & D). Over time, capillary refill can be visualized.

agents and subsequent reflow into tissue.

Complications associated with such measurements in 3D are addressed in this work.

Figure 1 shows a general schematic of contrast disruption and refill. An ultrasound beam is used to destroy contrast agent in all vessels in the imaging plane. The larger vessels with significant volume flow and high flow rates would quickly refill. The volumes of interest, however, are slower flow in the capillary bed. As the arterioles are filled, the contrast can be visualized, and eventually capillary refill will be seen.

Figure 2 depicts the dual-transducer imaging scheme.

For the sake of discussion, consider the case of a patient under constant drip infusion of ultrasound contrast agent. At steady state, the imaged blood is 100% contrast enhanced. By translating an ultrasound

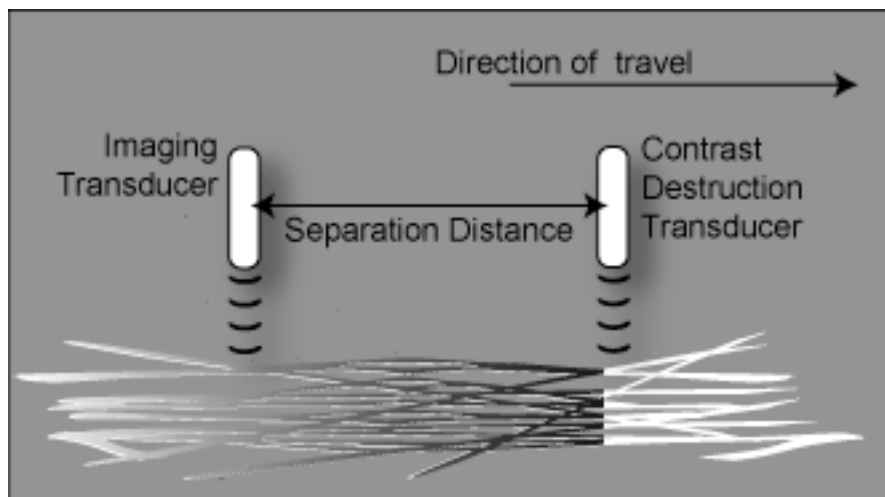


Figure 2. Schematic of dual-transducer method for monitoring capillary refill. The high intensity transducer is used to destroy contrast and create a zero-contrast-enhanced wavefront. The low intensity imaging transducer follows behind at some fixed time (distance). By sequentially scanning the same region using different delays, a refill-time map can be constructed for the volume.

transducer transmitting a sequence of high-intensity pulses, a wavefront of maximally broken contrast or “zero-contrast-enhanced” tissue is formed. Although the figure shows vessels virtually flowing in the same direction for simplicity, a model will be developed to describe the more “real-world” scenario of isotropically

distributed flow into and out of the particular volume of interest. The second transducer, which arrives at the same location at time 2, images the partially refilled volume. This process can be repeated multiple times using different delay settings between contrast destruction and imaging to estimate refill rates for every region in the overall imaged volume.

Specific Tasks:

In the originally proposal document, the approved statement of work included the five major tasks listed below:

Task 1 (months 1-6): Model input function of contrast agent destruction:

- (a) Generate mathematical flow model
- (b) Measure beam profile
- (c) Incorporate various profiles, flow, and scan rates

Task 2 (months 3-12): Assemble and test mechanical imaging scan system:

- (a) Design and construct mechanical translation system
- (b) Design and test electrical interface
- (c) Design and test interface software

Task 3 (months 13-24): Design and perform experimental assessment of imaging system design:

- (a) Evaluate performance on strict flow tube models
- (b) Evaluate performance on kidney phantom
- (c) Evaluate 3 point method of refill curve modelling

Task 4 (months 1-24): Develop and assess visualization and quantification software:

- (a) Verify flow model
- (b) Develop regional mapping software (*can start as soon as the project begins)
- (c) Develop and evaluate parametric histogram visualization scheme

Task 5 (months 13-36): Assess system and 3D imaging software on small patient population:

- (a) Recruit patients
- (b) Perform scans
- (c) Evaluate refill maps and parameterize
- (d) Test discriminators

Task 6 (months 30-36): Overall data analysis and write-up

At project's end, these tasks were addressed except for the assessment of the imaging system on an actual patient population. Quantification software (Task 4), shown in a previous report, could be modified to use data generated in schemes developed later. Task 3 was extensively expanded over the final years of the grant period, including 2 no-cost extension

periods, the final no-cost period being fairly lean. A significant portion of the analysis and discussion of these aspects appear in the papers "in press" and "under revision" in the appendix of this report. Additional analyses, which will appear in the revised paper submission, are described in the body of the report.

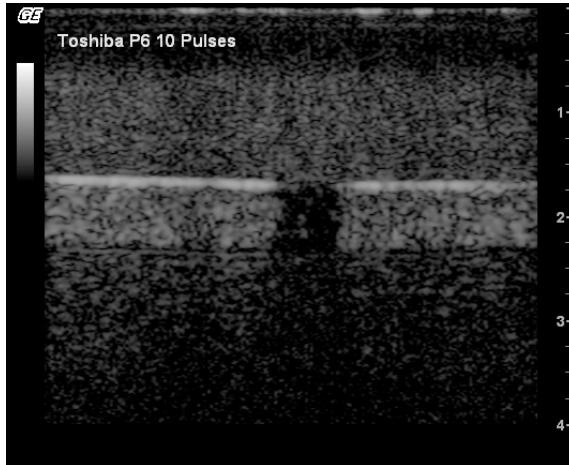


Figure 3. Image of contrast clearance zone thickness. This image, obtained from the imaging transducer at low power shows the 6 mm gap in stationary contrast generated by the clearance transducer after a series of 10 pulses. As such, the effective transducer separation was considered half of the gap (3 mm) less than the physical transducer separation.

Results:

A laboratory set-up and interface software was developed to implement the dual-transducer method described in the introduction and previous reports. The apparatus shown in Figure 4 of the "Demonstration of a Dual Beam Technique" paper in the appendix was used to translate the transducer pair at a constant rate. The distance between the two transducers was varied, and clearance/imaging sequences were performed over a 6.35 mm flow tube and kidney phantom. Contrast clearance zone thickness was imaged by applying multiple pulses to the tube and imaging longitudinally with low power as shown in Figure 3. This provided a "true" transducer separation distance for the analysis. The resulting imaged

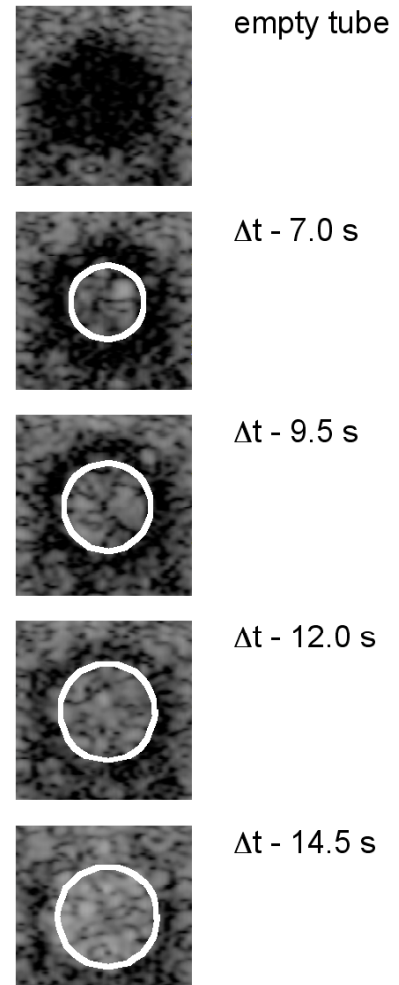


Figure 4. Sample planar images of tube flow. For the 0.040 mL/s flow rate, these images are a sample of those directly obtained in the transducer axial-lateral plane of the flow at a distance d of 16 mm for differing values of Δt . The circles of contrast have observed diameters respectively of 3.36, 4.47, 5.53, and 5.97 mm corresponding to theoretical values (outlined) of 3.67, 4.36, 4.76, and 5.02 mm with increases in Δt .

paraboloid is shown in the appendix. Figure 4 here presents corresponding cross-sectional views, which agree well with expected values. Again, overall results are discussed in the “Demonstration of a Dual Beam Technique” paper in the appendix.

Analysis of studies on fixed porcine kidney phantoms as described by Holmes and others [Holmes et al. 1984] initially resulted in the discussion shown in given in the “Application to

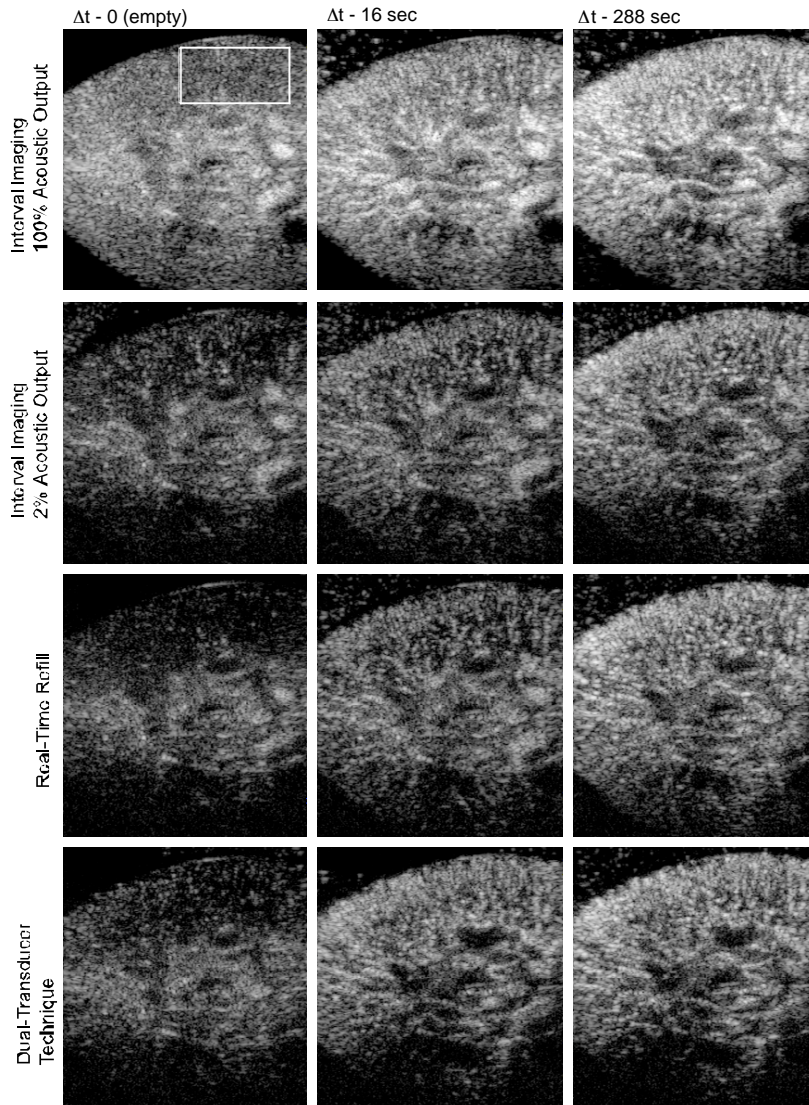


Figure 5. Representative transverse images obtained for a representative slice from preserved porcine kidney with interval imaging, real-time refill, and the dual transducer technique for refill times of 0, 16, and 288 sec. Images from real-time refill and dual transducer are obtained with the same acoustic settings as the 2% acoustic output interval imaging data. Interval imaging images obtained at 100% acoustic output are brighter because of the high transducer output used to obtain the images. Contrast clearance was obtained for both interval imaging cases and real-time refill using 50 pulses at 5 Hz at an acoustic output of 100%. The separate clearance transducer provided contrast clearance for the dual-transducer measurements. A rectangular window marks the region of interest in subsequent mean transit time comparisons.

Perfused Kidney Vasculature” paper in the appendix. As mentioned previously, the logistics of dehydrating and rehydrating these kidneys were initially problematic. As also continued to be an issue, the stability of contrast agent (Definity) was also problematic given the relatively long (20-30 minute) experimental protocol due to contrast exposure to atmosphere, suspension (stirring) issues, and various pumping parameters. Experimental results in the paper were thus interpreted with all of these factors in mind. regardless of interpretation, of particular interest are example cross-sectional images of the kidney during refill and longitudinal images extracted from the 3D volume as shown in Figures 3 and 7 of the paper, respectively. Cross-sectional images are reproduced here in Figure 5. With no correction or absolute calibration, we were able also to apply a method of parametric display of mean

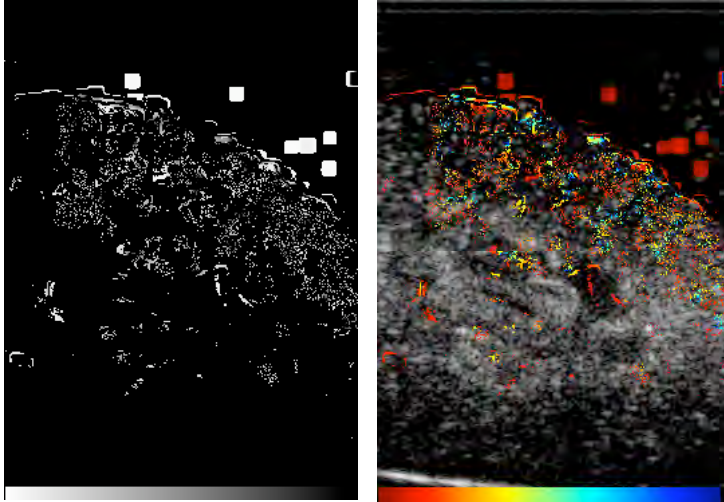


Figure 6. Initial parametric images of mean transit time (MTT) in porcine kidney. (Left) Grayscale bar white to nearly black represents shortest MTT (fastest refill) to longest MTT (slowest refill). Indeterminant points are black. (Right) Colorized MTT super-imposed onto original image, red to blue represents fastest to slowest refill. Efforts are underway to reduce the indeterminant regions, apparent primarily in the medullary region in this example. The scheme will also be used to display actual perfusion values as obtained in ongoing work.

transit times for the 3D volume. An example slice is shown in Figure 6. While we have reason to believe that these absolute times may have some inaccuracies, the mapping scheme is nonetheless valid, and will be modified to display final results when they are achieved.

In addition to the submitted and published works, ongoing preparations for a small clinical trial were being made. In terms of measurements, we have developed a scheme to and sufficiently fast transducer-holder apparatus (the latter funded under a separate grant) to modify the “dual-

transducer” technique to a “dual-sweep” technique. Figure 7 shows the transducer stage, which is able to traverse an area of interest in roughly 4 seconds. This will allow a “back-and-forth” sweeping to capture signal levels at appropriate time points, assuming early times are acquired slice-by-slice at minimal cost to the overall exam time.

In terms of analyses planned for the final trials, initial results of normalizing measured signals to a “threshold” intensity of the overall image (which presumably would represent 100% “blood”) looked promising. However, while threshold values appeared fairly stable with varying degrees of tissue refill, it became apparent that input contrast signals were not (as monitored in a major input vessel). We assumed that overall major vessel signals were lost or at least hidden in cumulative histograms. Figure 8 shows an example of contrast signal behavior in a major vessel as measured over time, in this case, in several “dual-transducer” runs. The time points represent the actual time when data was acquired over the course of the experiment.

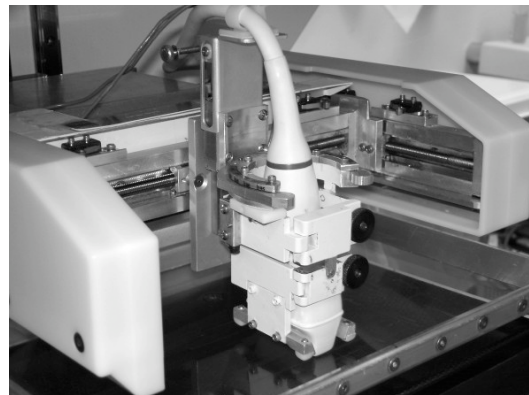


Figure 7. Single transducer apparatus. XY translation are both computer controlled, and imaging occurs through a mammographic style paddle for stability, although compression levels for the region of interest can be minimal. The “single-transducer-dual-sweep” scheme should be comparable to the investigated protocol.

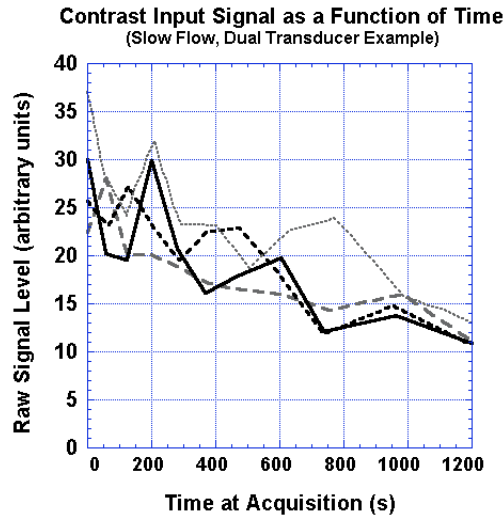


Figure 8, Contrast signal level decay over time. Presented are four intensity plots measured in the renal artery of an *in vitro* porcine kidney. In this case, the input flow rate was 1L/hr during dual-transducer acquisition. The abscissa represents the actual time data points were acquired rather than the *time coordinates* on the refill curve (see text).

Given the fact that the contrast signal changes over time, a scheme for normalizing the measured signal in the kidney was developed. The scheme is sensitive to the fact that a given major vessel signal may or may not be under the same conditions as the region of interest. In our case, it was important to correct for their relative locations in the image. Since the vessel is deeper, TGC, beam effects, and perhaps other influences affect the signal level of the lower lying vessel. To account for this, we have analyzed the signals at an upper and lower region of interest (ROI) over a broad range of contrast concentrations, simply acquired over the course of numerous experimental runs (Figure 9). In the end, we assume a relationship as follows: $I_{lower} = R \cdot I_{upper} \cdot 10^{(-0.1 \cdot KD \cdot I_{upper})}$, where K is a derived constant, D is

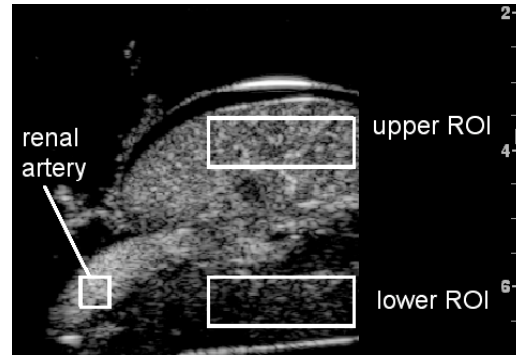


Figure 9, Regions of interest used to establish the relationship of upper and lower signal levels in the porcine kidney. The input major vessel is also highlighted.

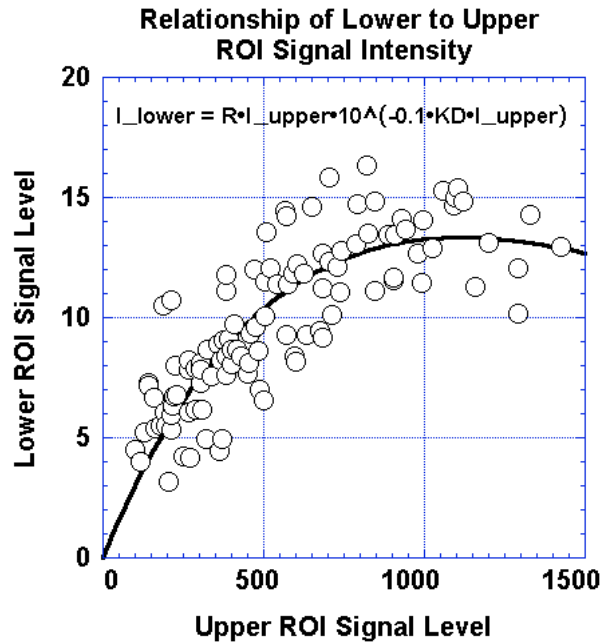


Figure 10. Model to establish a scaling factor R to account for beam effects present at lower depths. Data from numerous experiments of refilling kidney provided the points on the curve. We assume a relationship as follows: $I_{lower} = R \cdot I_{upper} \cdot 10^{(-0.1 \cdot KD \cdot I_{upper})}$, where K is a derived constant, D is distance, $KD \cdot I_{upper}$ is a simple expression of attenuation due to contrast agent, and R is a scaling factor accounting for any other differences between the upper and lower regions. $K \cdot I_{upper}$, then, is the attenuation coefficient for the “full” tissue (i.e. with contrast). Note the trend in data and modeled curve fit agree well.

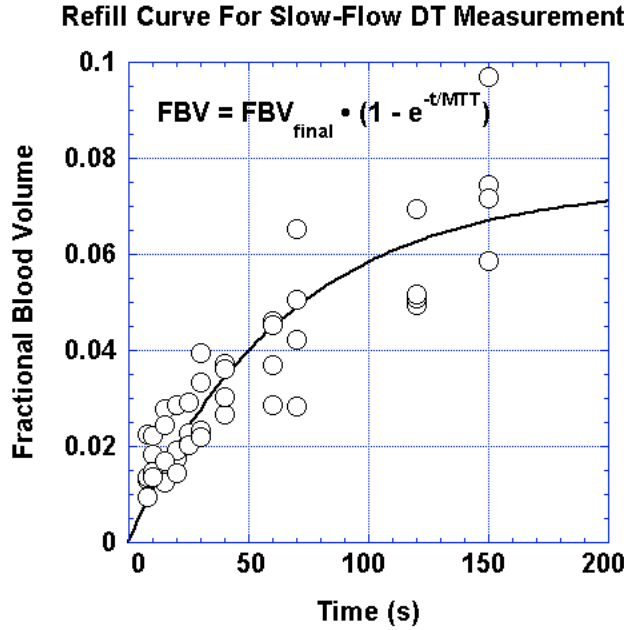


Figure 11. Sample refill curve of a cortex region of interest in a fixed porcine kidney. Corrected values yield a smooth fit and reasonable values of final fractional blood volume (~8%) and mean transit time (~65 seconds). See text for details.

is the intensity of the full upper ROI times K , then assuming an asymptotic mean signal level for the upper ROI of 1000, $\alpha_{full} = 0.8 \text{ dB/cm}$. With a fractional "blood" volume of 10% and our nominal input contrast concentration of 1:5000, the concentration of contrast in the imaged kidney is 10% times $1/5000 = 2 \times 10^{-5}$, or 0.02 ml/L. Such values (0.8 dB/cm at 0.02 ml/L) are at least consistent with the literature.

Using the corrections noted, refill curves for various cases of repeated studies including full power interval-imaging, low-power interval-imaging, and our dual-transducer technique were compared for a sample slice extracted from the 3D dual-transducer measurement. A sample refill curve is given in Figure 11. In this case, final fractional blood volume was roughly 8%, and mean transit time 65 seconds. Figure 12 shows the full complement of perfusion data. It is interesting to note variations in mean transit time among techniques, which was also present within given methods. Perfusion values, nonetheless, appear reasonable, with "fast-flow" cases always exceeding their "slow-flow" counterpart, and all values remaining within a statistically tight region. The implication is that despite fluctuations in input signal, input flow, and overall flow patterns within the kidney, the proposed method is as consistent as any other. The advantage, as described, is that we actually have 3D data throughout the kidney.

distance, $KD \cdot I_{upper}$ is a simple expression of attenuation due to contrast agent, and R is a scaling factor accounting for any other differences between the upper and lower regions. $K \cdot I_{upper}$, then, is the attenuation coefficient for the "full" tissue (i.e. with contrast). This relationship is shown in Figure 10 for the given data, high power interval-imaging data in this case. From the curve fit, the isolated value of R is 0.033, which can be used subsequently to scale the measured intensities of the major vessel signal. The value of KD for this particular case was 0.004.

As a check, for a distance D between ROIs of 2.5 cm (5 cm round trip), $KD = 0.004$; so $K = 0.0008$. As a check, if the attenuation coefficient of tissue with contrast agent (α_{full})

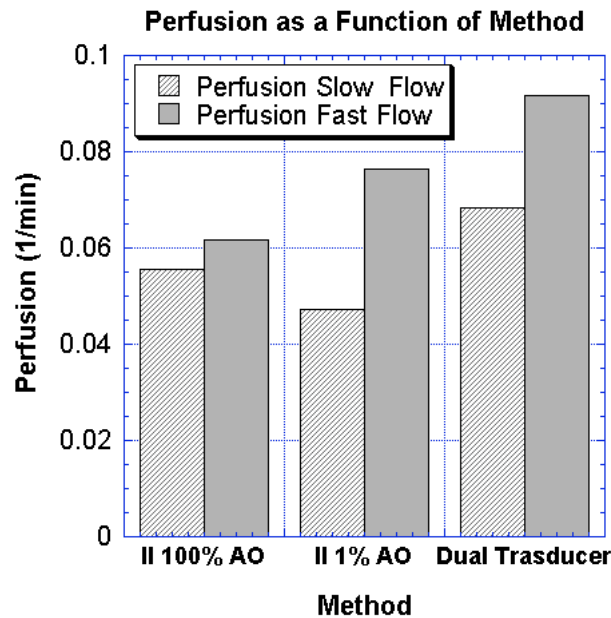
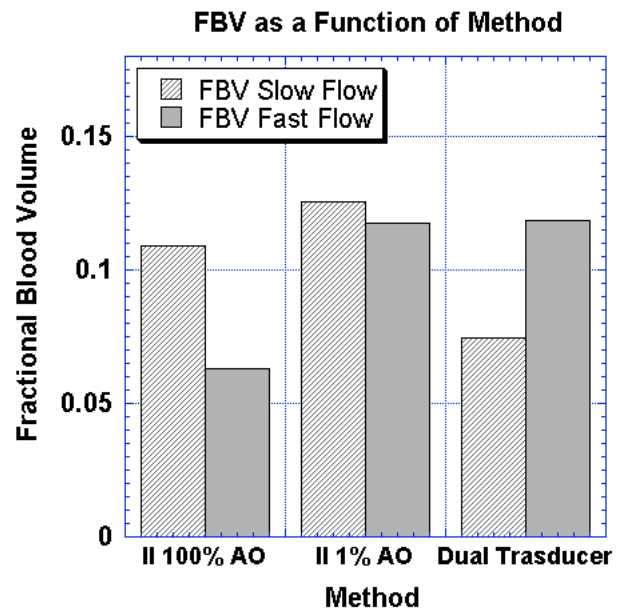
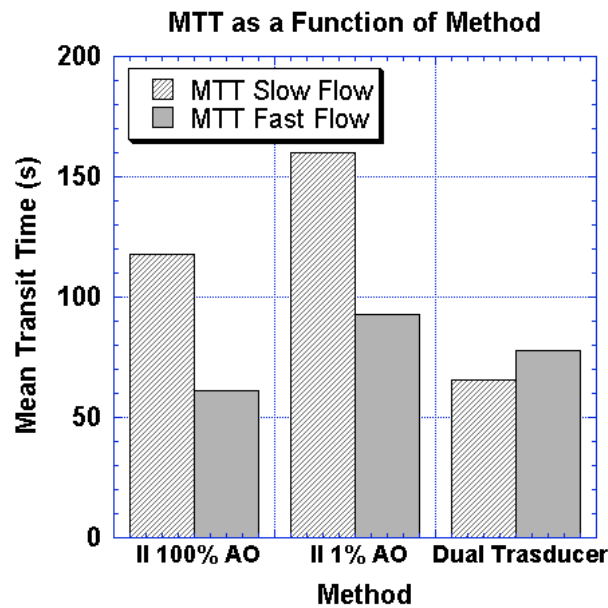


Figure 12. Perfusion measurement comparisons in a fixed porcine kidney. The three methods compared are interval-imaging under two different power levels and the investigated dual-transducer method. All data were corrected based on major vessel signals (see text). Although further investigation may be needed to determine why perfusion does not appear to scale with input flow rate in our particular region of interest, the three methods appear to yield comparable results. It should again be noted that the dual-transducer method provides similar data throughout the *volume* of interest, and these comparisons are simply samples extracted from the reconstructed volume.

It is unfortunate that the clinical trials were not undertaken: however, given the complexity of the method and analysis, we believe that we are near that point, and as noted, preparations have been made to that end.

Key Research Accomplishments

- Designed and completed mechanical scanning apparatus and its software interface. Additionally, a scheme was developed to migrate the "dual-transducer" method to a "dual-sweep" method with a single transducer apparatus.
- Performed extensive flow-tube experiments to determine reasonableness of dual-transducer method in the simplest case. This phase included quantifying a contrast "destruction zone" as a function of transducer output and number of pulses as well as correlating measured tube flow profiles with theoretical profiles, accounting for destruction zone characteristic. Additionally, variations from expected results were explained with a simplified mathematical tube model, accounting for time spent in the ultrasound beam.
- Experiments were extended to a fixed porcine kidney phantom after working out logistics of reproducibility of the model and developing an appropriate experimental pumping interface. Preliminary results showing refill characteristics of the kidney were compared for the dual-transducer versus the interval-imaging mode, and a parametric mapping scheme was developed.
- Extensive re-testing of kidney phantom provided insight into possible anomalies displayed in "real-time" refill scenarios, perhaps due to some destruction by low-power ultrasound pulses and possible coalescence of contrast agent bubbles. As such, comparison to "real-time" refill was dropped from the analysis due to (1) uncertainty regarding our "non-destructive" imaging scheme, and (2) its inherent difference in scheme from the other methods.
- Initial analysis of cumulative histograms of ultrasound scans showed promise in determining a value for %100 "blood" for each imaged slice. This method was eventually dropped due to ever-increasing threshold values for 100% "blood," imaged over time. While explainable, this would be inappropriate as a calibration / normalization value. Instead, signal level from an actual major vessel was used for normalization.
- Major vessel signals reflect the variation in contrast input level; however, corrections were required to account for vessel position relative to regions of interest. A preliminary model

was developed to account for positional differences between the reference and ROI, and results were applied to kidney refill images. The impact of this is that we should not only be able account for a varying input contrast signal, but may well be able to actually estimate perfusion.

- Such perfusion levels were in fact estimated with the described normalization scheme. Initial results on repeated kidney phantom studies for two input flow rates are promising, displaying reasonable perfusion values as well as reasonable estimates of contrast attenuation as a function of concentration.
- Refinements to the refill model are underway and preparations continue for clinical trial testing, which will be performed using internal funds and/or a follow-up grant.

Reportable Outcomes

The following publications stem from the grant, and are in press, submitted, or in revision. All are attached in the Appendix.

Peer Reviewed Papers

1. Chen NG, Fowlkes JB, Carson PL, LeCarpentier GL: Rapid 3D Imaging of Contrast Flow: Demonstration of a Dual Beam Technique. *Ultrasound in Medicine and Biology*, 2007 (in press).
2. Chen NG, Fowlkes JB, Carson PL, LeCarpentier GL: Rapid 3D Imaging of Contrast Flow II: Application to Perfused Kidney Vasculature. *Ultrasound in Medicine and Biology*, 2007 (submitted 2005, returned for revision, in revision).

Abstracts

1. LeCarpentier GL, Chen NG, Fowlkes JB, Carson PL: Preliminary Results of a New Method of 3D Ultrasound Contrast Agent Mapping of Vascular Anomalies for Characterization of Breast Cancer. Era of Hope Department of Defense Breast Cancer Research Program, Sep 25-28, Orlando, 2002, Proceedings P29-6.

2. LeCarpentier GL, Chen NG, Fowlkes JB, Carson PL: A New Dual-Transducer Method of Three-Dimensional Ultrasound Contrast Agent Imaging of Vascularity. (Proceedings of the 10th Congress of the World Federation for Ultrasound in Medicine and Biology) Ultrasound in Medicine and Biology, 2003, 29(5S): S53.
3. Chen NG, Fowlkes JB, Carson PL, LeCarpentier GL: Assessment of a 3D Dual-Transducer Ultrasound Contrast Agent Technique for Slow-Flow Vascular Imaging. Proceedings of the Biomedical Engineering Society Annual Meeting, Baltimore, 2005.
4. Chen NG, Fowlkes JB, Carson PL, LeCarpentier GL: A 3D Dual-Transducer Ultrasound Technique for the Assessment of Vascular Flow Using Contrast Agent Imaging. Proceedings RSNA 91st Scientific Assembly and Annual Meeting, Chicago IL, Dec 2005.
5. Chen NG, Fowlkes JB, Carson PL, LeCarpentier GL: A 3D Dual-Transducer Ultrasound Technique for the Assessment of Vascular Flow Using Contrast Agent Imaging. Proceedings of American Institute of Ultrasound in Medicine 50th Annual Conference, Washington, DC, 2006.
6. Chen NG, Fowlkes JB, Carson PL, LeCarpentier GL: 3D Perfusion Measurements Using a Dual-Transducer Ultrasound Contrast Agent. American Institute of Ultrasound in Medicine 51st Annual Conference, New York, NY, March 2007 (accepted).

Personnel

The following personnel received salary support over the course of the grant and no cost extension periods:

Gerald L LeCarpentier	Principal Investigator	Years 1-5
J Brian Fowlkes	Co-Investigator	Years 1-4
Nelson G Chen	Graduate Research Assistant	Years 1-5
Nadia Parkar	Computer Systems Assistant	Years 1-3
Ian Gibbs	Undergraduate Assistant	Year 1

Conclusions

The dual-transducer technique provides vascular refill information highly correlated to interval and real time imaging, while drastically reducing imaging time required for a 3D volume. The technique may provide measures of refill characteristics in small vessels and slow flow regions where Doppler methods fail. Nonetheless our previous Doppler analysis methods are well suited to contrast agent imaging quantification and breast mass characterization.

There is a time "cost" in obtaining refill data via any clearance/imaging scheme (whether it be interval imaging in 2D or the dual transducer method in 3D), and slow-flow regions may be affected by contrast decay. We have evaluated a method for estimating the signal level in 100% blood, which should provide us the ability to: (1) monitor fluctuations of input contrast signal level, and (2) calculate a real value for fractional blood volume. The latter, along with our mean transit time estimates will provide a measure of actual perfusion. Results to date are promising in this regard, with perfusion estimates consistent among measurement methods and consistent with reported values.

It is unfortunate that a small patient trial could not be undertaken within the scope of this project. Nonetheless, the technique appears nearly ready for such an extension in the near future. We continue to believe that perfusion measurements, especially in slow-flow and small vessel situations, will aid in the understanding of and early diagnosis of suspicious breast masses.

References

- Bhatti PT, LeCarpentier GL, Roubidoux MA, Fowlkes JB, Helvie M A, Carson PL: Discrimination of Sonographic Breast Lesions Using Frequency Shift Color Doppler Imaging, Age and Gray Scale Criteria. *Journal of Ultrasound in Medicine*, 2001, 20:343-350.
- Fowlkes JB, Sirkin DW, Ivey JA, Gardner EA, Rhee RT, Rubin JM, Carson PL. Transcutaneous interruption of ultrasound contrast agents for blood flow evaluation. *Investigative Radiology* 1998 Dec; 33(12):893-901.
- Holmes, K. R., Ryan, W., Weinstein, P. and Chen, M. M. A fixation technique for organs to be used as perfused tissue phantoms in bioheat transfer studies. *Advances in Bioengineering*. R. L. Spiker. New York, Amer. Soc. Mech. Eng. 1984; 9-10.
- LeCarpentier GL, Bhatti PT, Fowlkes JB, Roubidoux MA, Moskalik AP, Carson PL. Utility of 3D ultrasound in the discrimination and detection of breast cancer, *RSNA EJ*, 1999; <http://ej.rsna.org/ej3/0103-99.fin/titlepage.html>.

LeCarpentier GL, Roubidoux MA, Fowlkes JB, Krücker JF, Paramagul C, Hunt KA, Thorson NJ, Engle KD, Carson PL: Assessment of 3D Doppler Ultrasound Indices in the Classification of Suspicious Breast Lesions Using an Independent Test Population and a 4-Fold Cross Validation Scheme. *Radiology* 2002 (accepted).

LeCarpentier GL, Chen NG, Fowlkes JB, and Carson PL: Preliminary results of a new method of 3D ultrasound contrast agent mapping of vascular anomalies for characterization of breast masses. Era of Hope, Department of Defense (DOD) Breast Cancer Research Program (BCRP), Orlando FL, September 25-28 2002, P29-6.

LeCarpentier GL, Chen NG, Fowlkes JB, and Carson PL: A new dual-transducer method of 3D ultrasound contrast agent imaging of vascularity. AIUM-hosted 10th Congress of the World Federation for Ultrasound in Medicine and Biology, 2003 (accepted).

Lee WJ, Chu JS, Huang CS, Chang MF, Chang KJ, Chen KM. Breast cancer vascularity: color Doppler sonography and histopathology study. *Breast Cancer Research And Treatment* 1996; 37(3):291-8.

Madjar H, Prompeler HJ, Sauerbrei W, Wolfarth R, Pfeleiderer A. Color Doppler flow criteria of breast lesions. *Ultrasound in Medicine and Biology* 1994; 20(9):849-58.

Peters-Engl C, Medl M, Mirau M, Wanner C, et al. Color-coded and spectral Doppler flow in breast carcinomas--relationship with the tumor microvasculature. *Breast Cancer Research And Treatment* 1998 Jan; 47(1):83-9.

Porter TR, Li S, Kricsfeld D, Armbruster RW. Detection of myocardial perfusion in multiple echocardiographic windows with one intravenous injection of microbubbles using transient response second harmonic imaging. *Journal of the American College of Cardiology* 1997; 29(4):791-9.

Porter T, Xie F. Transient myocardial contrast after initial exposure to diagnostic ultrasound pressures with minute doses of intravenously injected microbubbles. Demonstration and potential mechanisms. *Circulation* 1995; 92(9):2391-5.

Rhee RT, Fowlkes JB, Rubin JM, Carson PL. Disruption of contrast agents using pulsed ultrasound. *J. Ultrasound Med* 1998; 16:S97.

Wei K, Jayaweera AR, Firoozan S, Linka A, Skyba DM, Kaul S. Quantification of Myocardial Blood Flow With Ultrasound-Induced Destruction of Microbubbles Administered as a Constant Venous Infusion. *Circulation* , 1998; 97(5):473-483.

APPENDIX



● *Original Contribution*

RAPID 3D IMAGING OF CONTRAST FLOW: DEMONSTRATION OF A DUAL BEAM TECHNIQUE

N. G. CHEN,* J. B. FOWLKES,*[†] P. L. CARSON,*[†] and GERALD L. LECARPENTIER[†]

*Departments of Biomedical Engineering and [†]Radiology, University of Michigan, Ann Arbor, MI, USA

(Received 7 November 2005; revised 21 October 2006; in final form 26 October 2006)

Abstract—Perfusion imaging in a 3D volume using ultrasound contrast agent may improve vascular characterization compared with 2D imaging. Conventional 3D acquisition requires excessive scan time. A dual transducer technique using conventional systems has been introduced that allows 3D imaging of contrast dynamics with drastically reduced scan times (LeCarpentier et al. 2003). Two transducers are translated across a volume where the leading transducer effects contrast clearance and the following transducer images at desired contrast refill times. With 2D arrays that allow simultaneous clearance and imaging pulses, scan times could be further reduced and the need for two transducers eliminated. The dual transducer technique was demonstrated on a tube phantom, with observed contrast profiles matching those expected. Measured center velocities of (\pm std dev) 1.46 ± 0.21 and 2.25 ± 0.5 did not statistically differ from expected values of 1.75 and 2.50 (all mm/s), ($p > 0.05$). This technique is introduced for rapid acquisition of 3D contrast refill images. (E-mail: gllec@umich.edu) © 2006 World Federation for Ultrasound in Medicine & Biology.

Key Words: Contrast refill, Perfusion, Blood flow, Imaging, Vasculature, Angiogenesis.

INTRODUCTION

Earlier studies have suggested that malignant masses have deviant vasculature including thin-walled blood vessels, increased microvessel density, disordered neo-vascularization penetrating the mass, arteriovenous shunting and other histologic findings (Folkman and Beckner 2000; Vaupel et al. 1989; Weidner et al. 1991). Visualization, mapping and quantification of the blood flow within and surrounding tumors may provide a means for differentiating between benign and malignant masses (Bell et al. 1995; Cosgrove et al. 1990, 1993; Delorme et al. 1995; Kedar et al. 1995, 1996; Lee et al. 1996; Peters-Engl et al. 1998; Vaupel et al. 1989). Extension into 3D may further improve the ability of discriminating between benign and malignant masses (Carson 1997). Additional Doppler volumetric scans with various quantitative blood flow measures have been conducted in a variety of organs. Examples include breast (Bhatti et al. 2001; Carson et al. 1998, Hochmuth et al. 2002), prostate (Moskalik et al. 2001a, 2001b;

Potdevin et al. 2001), uterus (Jokubkiene et al. 2006), placenta (Merce et al. 2005) and ovary (Chan et al. 2003). Mehta et al. (2004) have reviewed various studies which show the advantages of 3D ultrasound with and without contrast enhancement relative to 2D scans in the detection and staging of prostate cancer.

Extensive evaluation of ultrasound contrast agents for the measurement of blood flow has been previously performed (Porter and Xie 1995; Porter et al. 1997; Wei et al. 1998) and is related to the refill of contrast agent into the tissue after contrast clearance. In early studies, refill data were obtained using interval imaging (Kamiyama et al. 1996, 1999; Ohmori et al. 1997; Wei et al. 1998), where a plane is cleared of contrast and allowed to refill for a given time. The process is repeated with different times to gather the images at various refill times. Signal intensities for regions-of-interest encompassing the image are plotted against their refill times. Fitting these data using a model for refill gives the mean transit time (MTT) of each region-of-interest. Combining the MTTs for regions throughout the image produces a refill map. Subsequent development of low-power, essentially nondestructive, pulse sequences enables the measurement of refill curves in real time after clearing the plane, in what is termed real-time refill imaging (Porter et al. 1999; Simpson et al. 1999).

Address correspondence to: Gerald L. LeCarpentier, PhD, University of Michigan Department of Radiology, Basic Radiological Sciences, 200 Zina Pitcher Place Rm 3315, Ann Arbor, MI 48109-0553, USA. E-mail: gllec@umich.edu

Both of these techniques are capable of gathering refill data for a single imaging plane in a reasonable period. However, a tumor is a three-dimensional mass and extending data collection to such volumes is impractical because of tremendous time requirements. Acquisitions that require a modest time t for a single plane may become unfeasible in 3D, since every single imaging plane constituting part of the volume would require t to acquire. The volume would also need to be perfused with contrast agent during this entire period. Ideally, the further development of two-dimensional arrays would allow the imaging of 3D volumes without the need for mechanical translation at frame rates comparable with those available with conventional 1D transducers (Hoskins 2002). However, their development has been problematic, with large storage requirements and large number of required digital channels.

THEORETICAL CONSIDERATIONS

Laminar viscous fluid flow through a straight circular cylinder has a well-known parabolic velocity profile given by

$$u(r) = V_c \left[1 - \left(\frac{r}{R} \right)^2 \right], \quad (1)$$

where $u(r)$ is the flow velocity at radius r from the center, V_c is the center velocity and R is the tube radius. This velocity profile is independent of time.

Consider the case presented in Fig. 1. If, at a given starting position along the cylinder, one selects volume elements at uniform position $p = 0$ at time $t = 0$ for all r , then the position of the elements composing the front $p(r,t)$ is simply $tu(r)$. The front continually stretches with increasing t . Substitution provides

$$p(r,t) = tu(r) = tV_c \left[1 - \left(\frac{r}{R} \right)^2 \right]. \quad (2)$$

Letting d represent the distance along the tube where the imaging transducer samples the contrast agent radii, with $d = 0$ being the initial uniform position of the front at $t = 0$, solving for the radius r as a function of d gives the following expression for $r(d,t)$

$$r(d,t) = R \sqrt{1 - \frac{d}{tV_c}}. \quad (3)$$

Since the dual-transducer technique translates the imaging transducer along the tube after contrast clearance, contrast radii are measured as functions of d and t . Therefore, this model allows the testing of the dual-transducer technique in imaging three-dimensional flows via a comparison of observed and predicted radii. The actual profile predicted under these imaging conditions

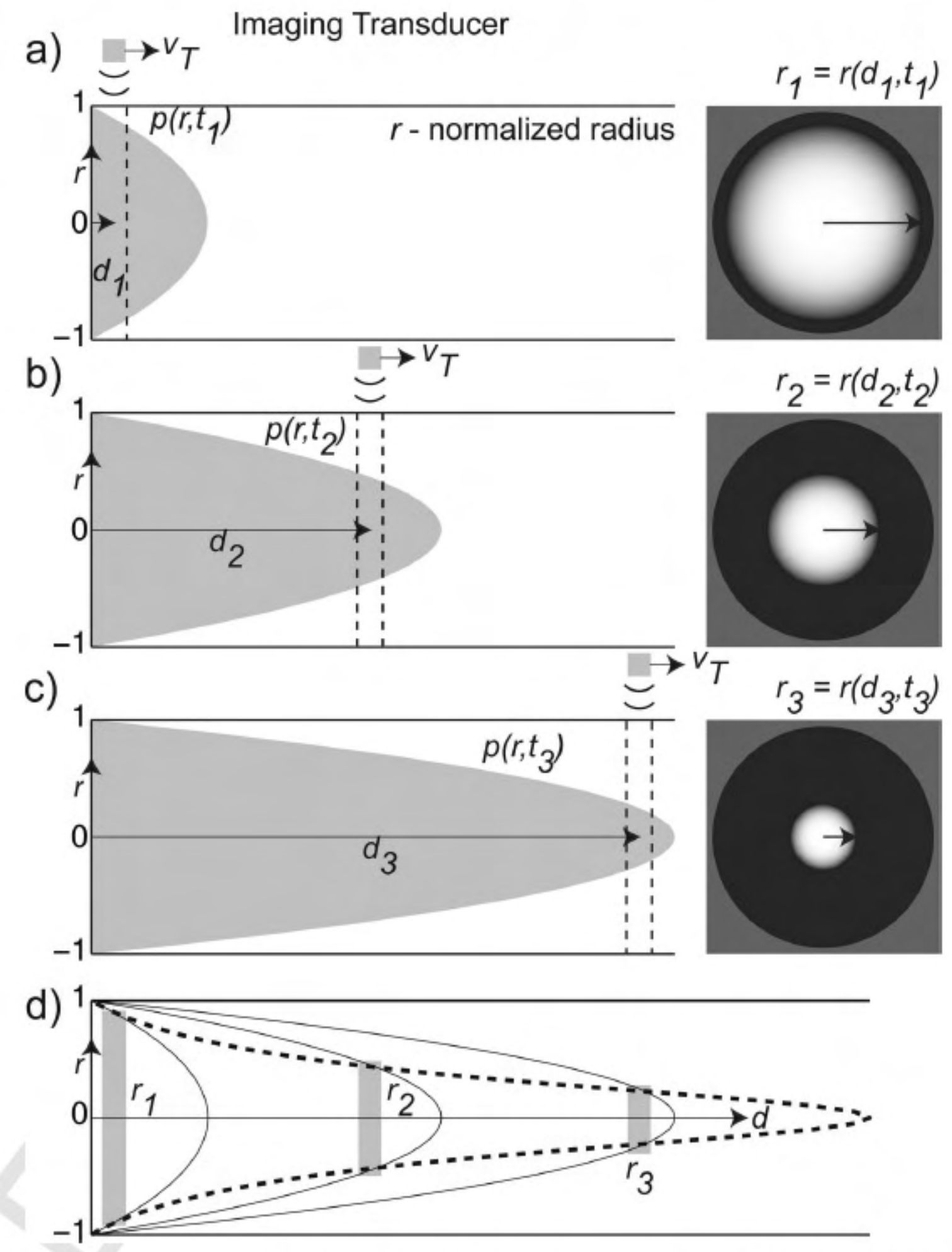


Fig. 1. Dual transducer tube flow dynamics. (a) At a given time t_1 , contrast refilling the tube cleared previously by the clearance transducer forms a parabolic profile. The imaging transducer images a slice of the profile in cross-section at position d_1 . Within that cross-section, the refilled contrast has a radius r_1 . (b) and (c) The contrast profile remains parabolic as the tube refills. At times t_2 and t_3 , the cross-sections are imaged at positions d_2 and d_3 , respectively. Even although the contrast profile at any instant in time t is parabolic, the measured radii r are taken of contrast profiles at different times. (d) If the transducer translation velocity v_T were to be much larger than the flow velocity, the contrast profiles at each time would not substantially evolve and r would solely be a function of the position d and the initial delay time between contrast clearance and profile imaging. However, there is a simple relationship for $r(d,t)$ (derived in the text) when the contrast profiles evolve significantly, given by $r(d,t) = R\sqrt{1 - d/tV_c}$, where R and V_c are, respectively, the tube radius and center flow velocity. Assembling the measured radii from an evolving contrast profile produces a predictable "time-dilated" parabola (shown by the dashed line).

can be considered to be a "time-dilated" parabola, as given by eqn 3 and shown in Fig. 1.

For a given transducer translation velocity v_T and transducer separation s (known from the dual-transducer configuration) and an observed time-dilated parabola, one could derive the center flow velocity V_c by substituting the expression $v_T t - s$ for d in eqn 3, reducing $r(d,t)$ to a function of only t

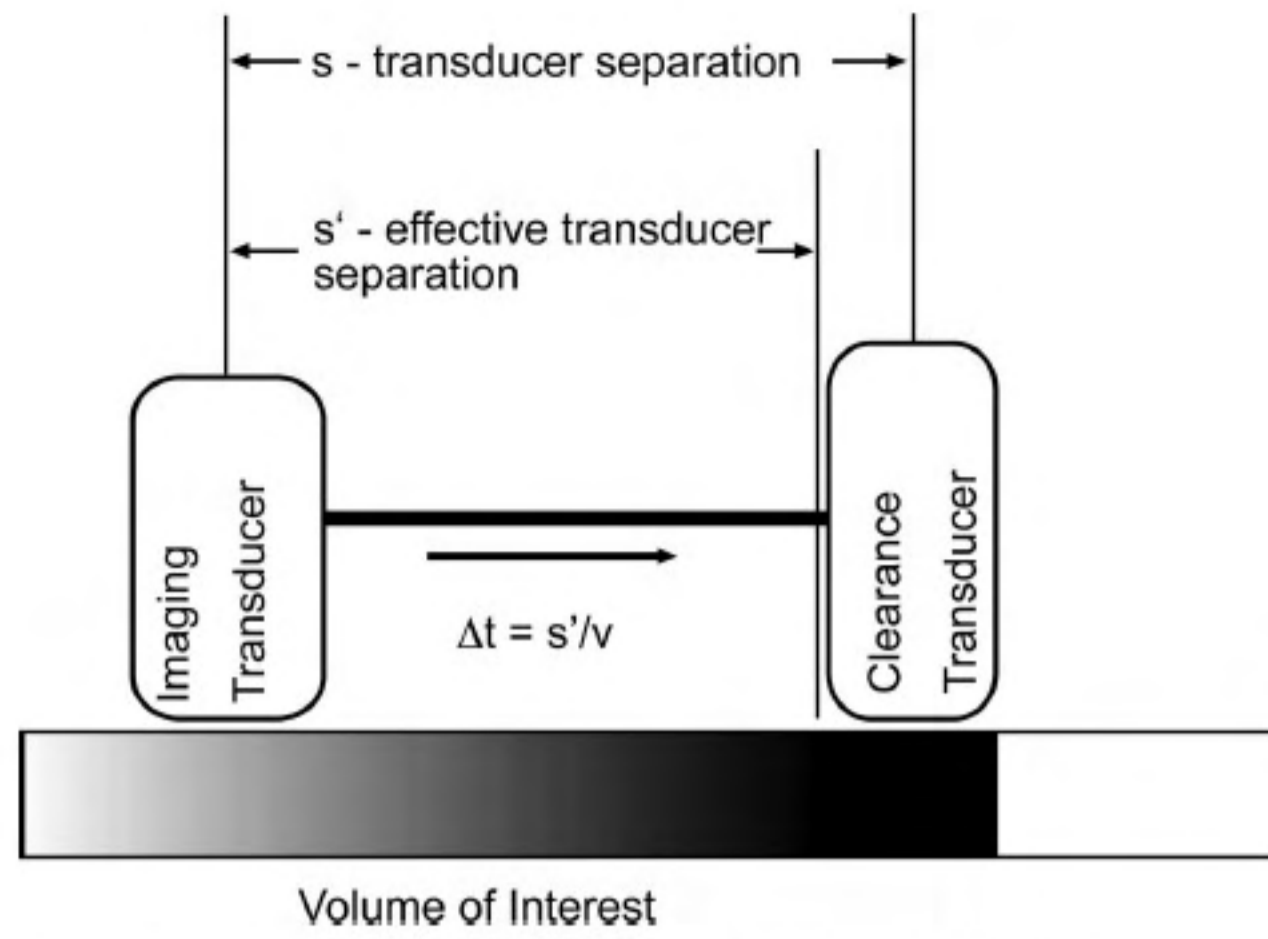


Fig. 2. Dual transducer method schematic. Each transducer is assigned a separate task, with the clearance transducer translated over the tissue ahead of the imaging one. The clearance transducer is operated at sufficient power and pulse repetition frequency (PRF) to clear the volume-of-interest of contrast agent during each sweep. The imaging transducer is operated in a minimally-destructive mode and it reads the amount of contrast agent that has refilled since contrast clearance. Both transducers are swept through the volume-of-interest at constant velocity v . Based on the separation distance s , the refill associated with a specific interval Δt can be measured. Due to significant clearance zone thickness, s' is less than s , the transducer center-to-center distance. Additional delay can be added by pausing the sweep after clearance and before imaging.

$$r(d, t) = R \sqrt{1 - \frac{d}{tV_c}} \rightarrow r(t) = R \sqrt{1 - \frac{v_T t - s}{tV_c}}. \quad (4)$$

One can fit all the measured radii at their known times t to the expression $r(t)$ and estimate the parameter V_c for any given experiment. Comparing the estimated and known V_c values (based on flow rates) provides a measure of the accuracy of the dual transducer technique.

METHODS

A technique is described which makes three-dimensional contrast data collection more practical with 1D transducers. The technique is demonstrated by sweeping a transducer pair, composed of a clearance transducer and a low-power imaging transducer as a unit at velocity v over a contrast perfused tissue volume. The clearance transducer causes contrast to be cleared in the swept volume. Since contrast is continually perfusing, the emptied volume immediately begins to refill with contrast. The imaging transducer reaches the location previously occupied by the clearance transducer in time Δt for all positions. As Δt has elapsed regardless of the position along the volume, the imaging transducer images the state of contrast refill at all positions for time Δt after each sweep. Longer Δt values can be obtained by pausing the sweep immediately before the imaging transducer begins entering the volume-of-interest. A schematic of

the method used to demonstrate the technique is shown in Fig. 2. Here, two transducers are used but the procedure could be applied for any approach in which separate clearance and imaging sequences can be combined, with the logical extension to 3D imaging systems.

A series of sweeps with varying Δt allows collection of refill images for the volume. The dual-transducer technique requires only slightly more time than single slice interval imaging acquisition, thereby making the visualization and mapping of three-dimensional volumes practicable in comparison with single-slice acquisition techniques (see Table 1 and the Appendix). Slice separation is determined by both acoustic frame rate and translation velocity. Under the normal operating limits of the translation system and scanner, the number of acquired image planes over the volume-of-interest does not affect the overall acquisition time.

In order to test the effectiveness of the dual-transducer technique for high-speed contrast imaging, flow through a tube phantom was imaged. A cylindrical tube was embedded within tissue-mimicking foam and contrast agent was pumped through at known rates. Since the flow profile through the cylinder is theoretically known,

Table 1. Comparison of required total time for interval imaging, real-time refill and the dual transducer technique.

Constant parameters used to compute the times are a transducer translational velocity v_T of 6 mm/s, a transducer separation of 60 mm and a volume-of-interest thickness of 40 mm. Chosen time-points for interval imaging and the dual-transducer technique are (in s) 10, 20 and 30 for three time points, with the additional points 15 and 25 for five time points. Real-time refill imaging acquires all time points continuously up to the maximum time point. Transducer translation time is negligible for real-time refill and interval imaging (~ 6.5 s) and is covered in the rounded times. For the dual-transducer case, the transducer pair is moved back to the starting position after the acquisition of each time-point, except for the final one. Time required to clear contrast is negligible (< 2 s) for both interval imaging and real-time refill acquisition. Note that using the dual-transducer method causes a dramatic reduction in the time required to image a three-dimensional volume. Since the dual-transducer technique's time requirement is independent of the slice thickness, image slices could be acquired as closely together as necessary without requiring additional time, subject only to the imaging transducer frame rate, unlike traditional techniques

Slice separation (mm)	Number of time points (interval and dual transducer imaging)	Interval imaging	Dual-transducer technique	Real-time refill
0.5	3	80 min	1 min 53 s	40 min
1	3	40 min	1 min 53 s	20 min
2	3	20 min	1 min 53 s	10 min
1	5	67 min	3 min 20 s	20 min

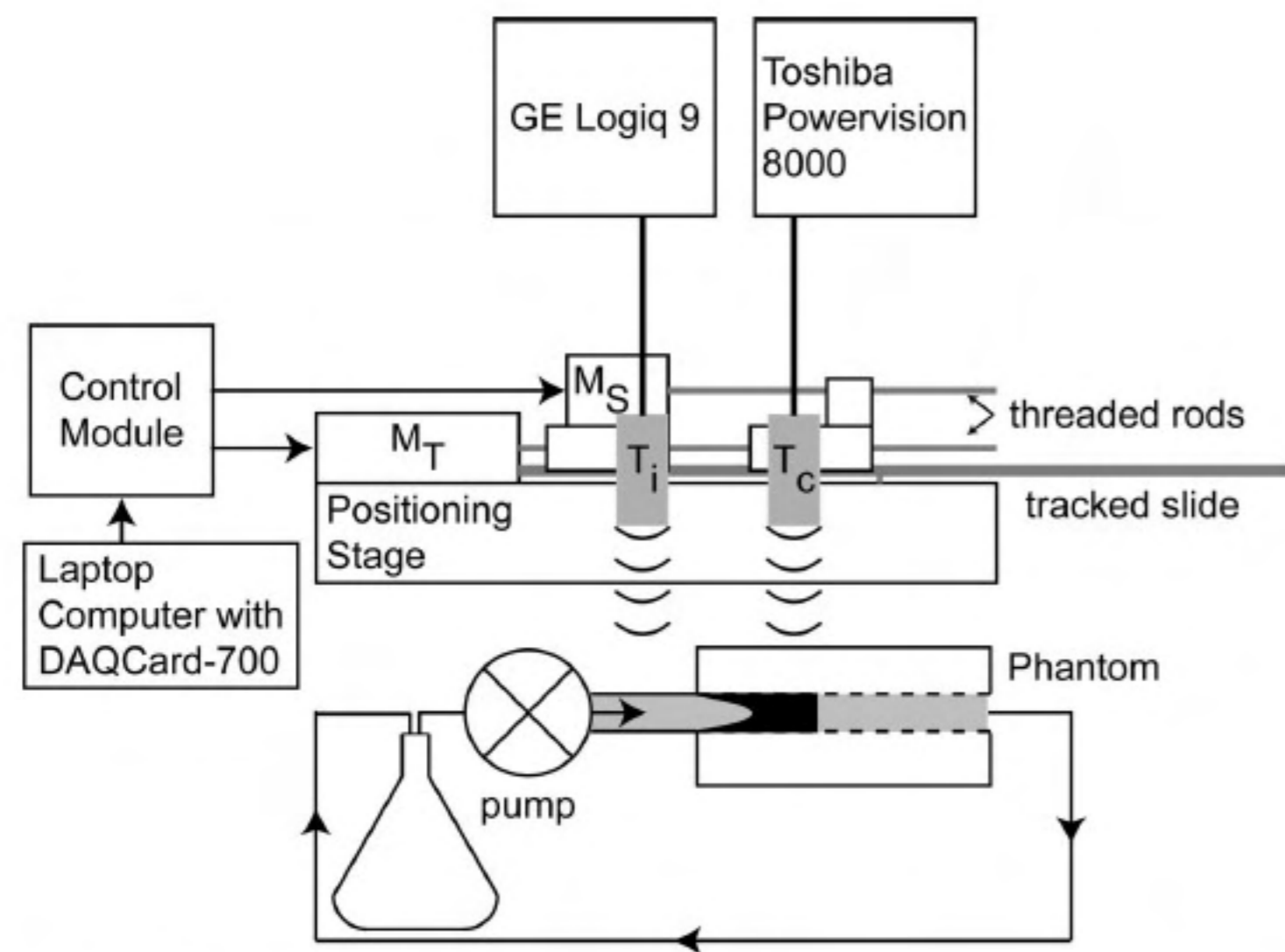


Fig. 3. Schematic of dual-transducer apparatus and experimental set-up. The dual-transducer apparatus consists of a dual-transducer positioning stage, which consists of translation (M_T) and separation (M_S) motors. Each motor turns a threaded rod, which translates a platform that contains a transducer holder. The platforms translate within the tracked slide. Motors are connected to a power control module, which contain the electronics driving the motors. The control module is linked to a laptop computer through the DAQCard-700. Using LabVIEW scripts, transducers are translated as required. The transducers are positioned above the phantom being scanned, with the clearance transducer (T_c) positioned at the edge of the volume-of-interest. The phantom is continuously perfused with dilute (1:5000 concentration) contrast pumped from a stirred flask.

one can compare measured three-dimensional profiles with those expected from theory.

All scans were conducted within a water tank lined with sound absorbent rubber and filled with water that had been allowed to come to gas saturation. A schematic of the overall experimental set-up is shown in Fig. 3. The phantom was mounted beneath the water on a stand and secured with two rubber bands. A dual transducer assembly is shown in Fig. 4 and was constructed using two stepper-motors and controls (Microkinetics Corporation, Kennesaw, GA, USA). The motors were controlled from a laptop computer through LabVIEW (National Instruments Corporation, Austin, TX, USA) scripts and the DAQCard-700 (National Instruments). The scripts allowed control of both transducer separation and translation along the transducers' elevational direction. The transducer assembly was mounted upon a second stand that placed the transducers above the phantom being scanned.

To build the tube phantom, a block of tissue-mimicking foam (S80: Crest Foam Industries, Inc., Moonachie, NJ, USA) was saturated with water and frozen in order temporarily to harden the block sufficiently for drilling. A circular hole with a diameter of 6.4 mm was drilled through the block and the foam was subsequently allowed to thaw. Next, a thin-walled

(0.79 mm) latex rubber tube with a 6.35 mm inner diameter (Kent Elastomer, Kent, OH, USA) was threaded through the block, with sufficient additional tubing (~ 20 times diameter) on both ends of the block to dampen transitional flow effects due to connections. The foam block was degassed before use by submersion in boiling water and subsequently allowed to cool, after which the phantom was maintained under water at all times.

The tube phantom was connected to form a recirculating flow system using IV (IV) tubing. A variable rate IV pump (IVAC 560, IVAC Corporation, San Diego, CA, USA) drove the flow. All flow originated and terminated at a stirred flask containing a contrast suspension (Definity: Bristol-Myers Squibb Medical Imaging, at a 1:5000 dilution in water). The suspension was continuously circulated through the phantom.

A Toshiba Powervision 8000 scanner (Toshiba America Medical Systems, Tustin, CA, USA) with a 3.75 MHz (PVN-375AT) transducer in harmonic mode (power setting of P6 giving a $MI = 0.2$ with a frame rate of 10 Hz) was used for contrast clearance. A GE Logiq 9 scanner (General Electric Healthcare, Milwaukee, WI, USA) with a 7L transducer in CPI (coded phase inversion) mode was used to image. Since the clearance transducer has a significant contrast disruption zone, as indicated in Fig. 2, the effective clearance width in the

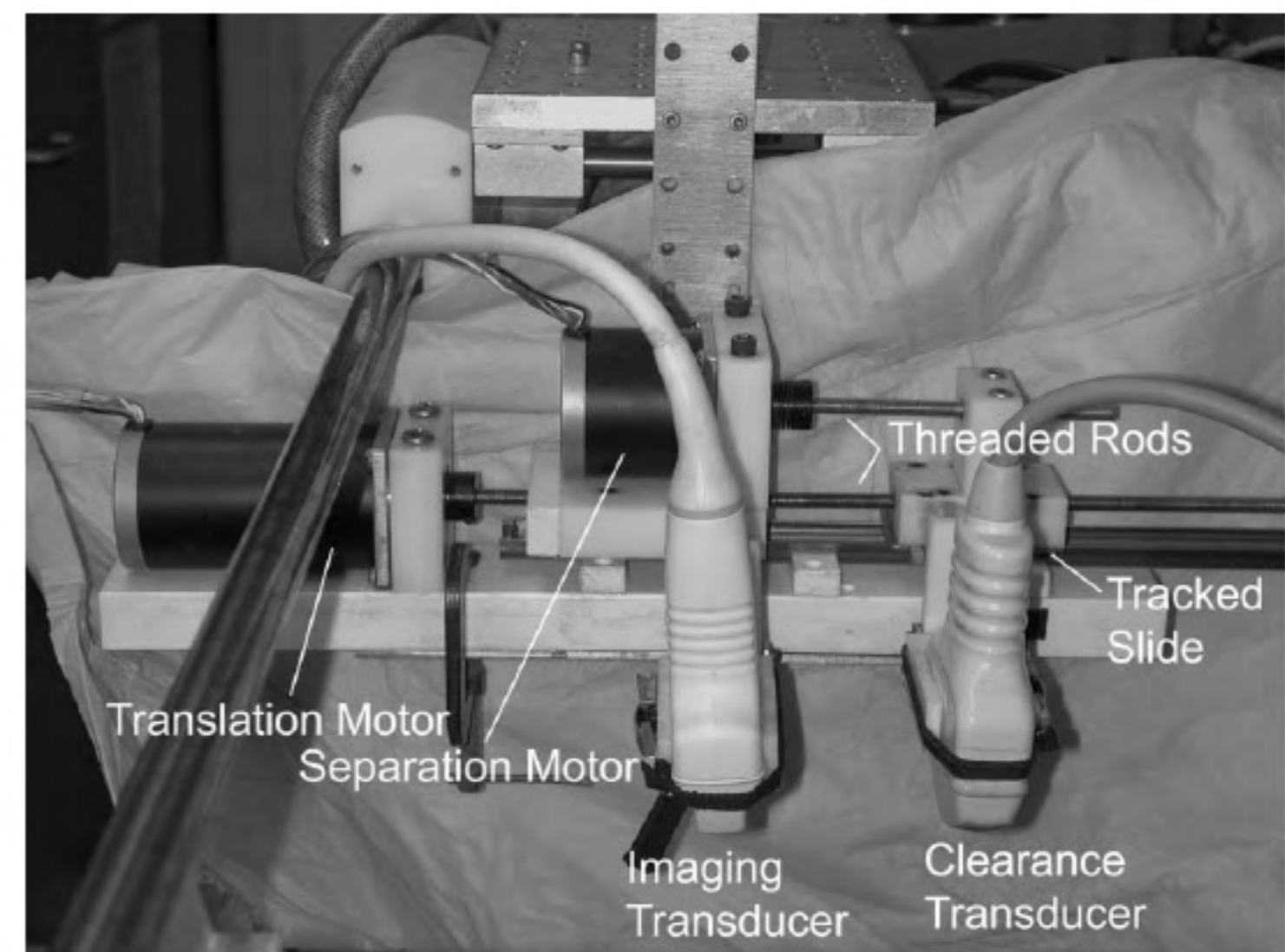


Fig. 4. Photograph of the constructed dual-transducer apparatus. Two stepper motors turn two threaded rods parallel to each other to move the ultrasound transducers, which are held by the transducer holders shown. Transducer holders translate on a guided slide (400L: THK Corporation Japan). The separation motor, mounted upon a stand, adjusts transducer separation. The stand, in turn, is translated by the larger translation motor, which controls the sweeps over the volume-of-interest. Imaging and clearance transducers are mounted as shown. The complete apparatus was placed above a rubber-lined water tank upon a stand and cables connected the motors to a control box (not shown), which provided drive power and was, in turn, controlled by a laptop computer using the DAQCard-700 and LabVIEW scripts.

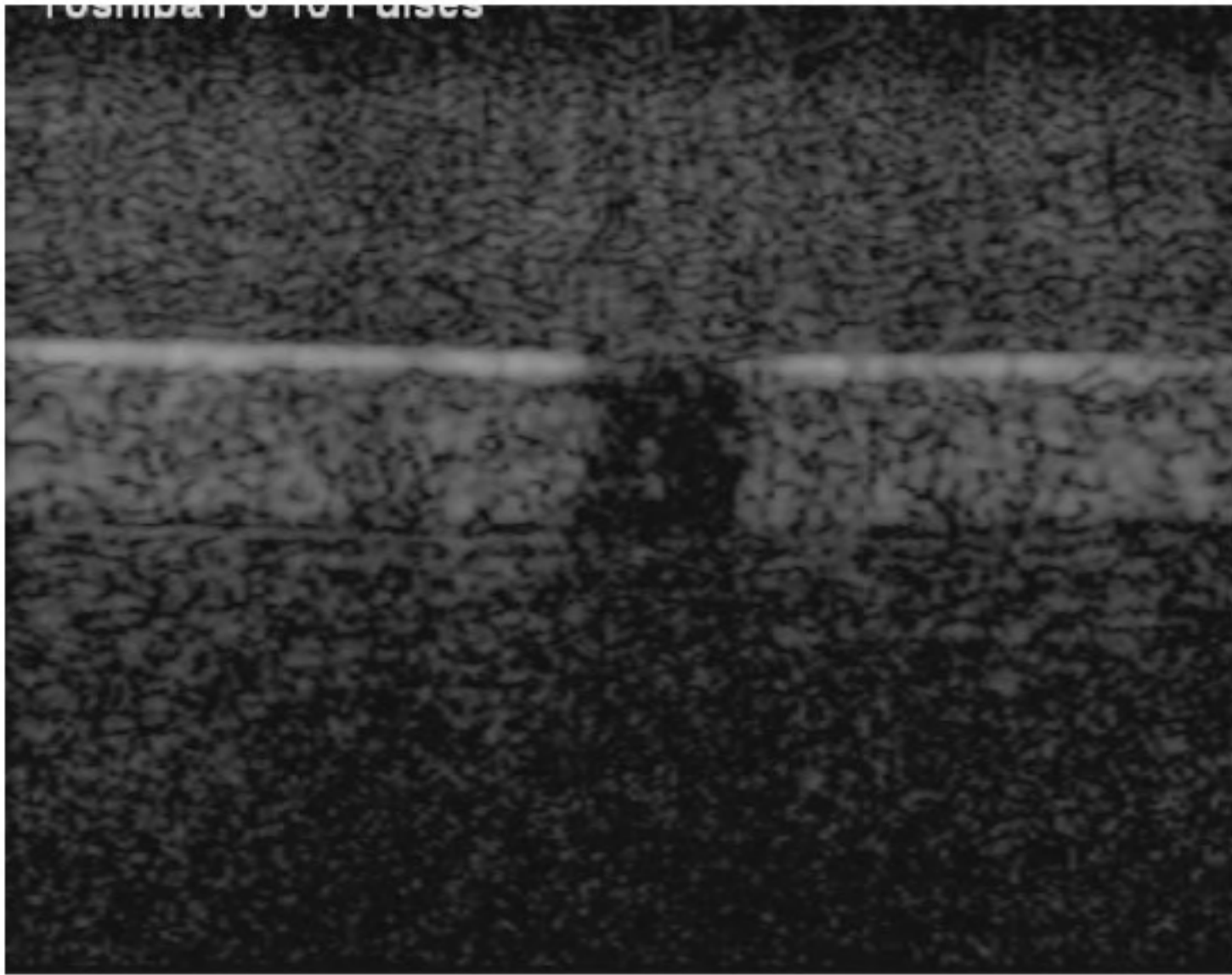


Fig. 5. Image of contrast clearance zone thickness. This image, obtained from the imaging transducer at low power, shows the 6 mm gap in stationary contrast generated by the clearance transducer after a series of 10 pulses (settings described in the text). The size of the gap asymptotically approaches this value with clearance transducer pulses. As such, the effective transducer separation was considered to be half of the gap (3 mm) less than the physical transducer separation.

elevational direction of the clearance transducer was measured by stopping the pump, applying a series of frames and imaging laterally the contrast gap produced using the imaging transducer at low-power (1% acoustic output power setting giving a $MI = 0.06$, focus at 10 mm). Calculations of Δt were based on the distance from the edge of contrast clearance to the center of the imaging transducer. The limit of the clearance width as the number of frames increased without bound was noted as 6 mm and used as the effective width, as seen in Fig. 5. As such, the effective transducer separation for each scan was considered 3 mm less than the physical transducer separation.

The dual transducer system was used to image the tube phantom at two different flow rates (1.75 and 2.50 mm/s peak velocity) with effective transducer separations of 42, 57, 72 and 87 mm. The imaging transducer axial focus was changed to 20 mm to place it closer to the tube within the phantom. Cross-sectional images of the tube phantom were acquired and assembled. Images through the tube center in the lateral-elevational plane were then extracted from the reconstructed 3D imaging volume and scaled appropriately for the transducer translation velocity v_T (6 mm/s) and frame acquisition rate (19 Hz). Imaged contrast was subsequently compared with expected “time-dilated” parabolae. Observed and expected profiles were compared visually and quantified by fitting the observed profiles to their corresponding measures of center velocity v_c provided by eqn 4. The lateral-elevational plane was selected for comparison to

avoid asymmetric effects of overlying attenuation on the contrast profile. In addition, overlying attenuation due to contrast is eliminated at the profile edge and a constant point-spread function is maintained throughout the plane.

RESULTS

For a given cross-sectional plane imaged over time, one would expect a series of enlarging discs of contrast, as depicted in Fig. 6, which shows a single plane ex- F6
tracted from three-dimensional data sets acquired using the dual transducer technique, with circles outlining the expected discs. Representative composite images of time-dilated parabolae assembled from the cross-sec-

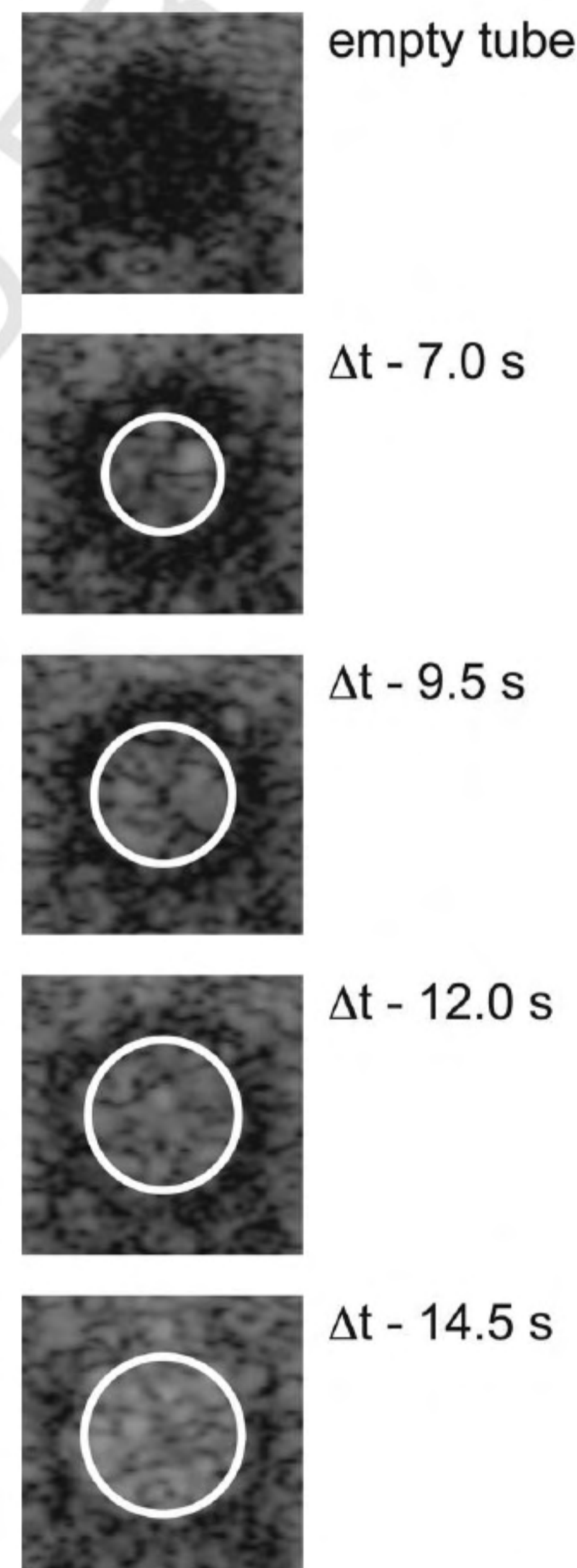


Fig. 6. Sample planar images of tube flow. For the 0.040 mL/s flow rate, these images are a sample of those directly obtained in the transducer axial-lateral plane of the flow at a distance d of 16 mm, for differing values of Δt . The circles of contrast have observed diameters, respectively, of 3.36, 4.47, 5.53 and 5.97 mm, corresponding to theoretical values (outlined) of 3.67, 4.36, 4.76 and 5.02 mm with increases in Δt .

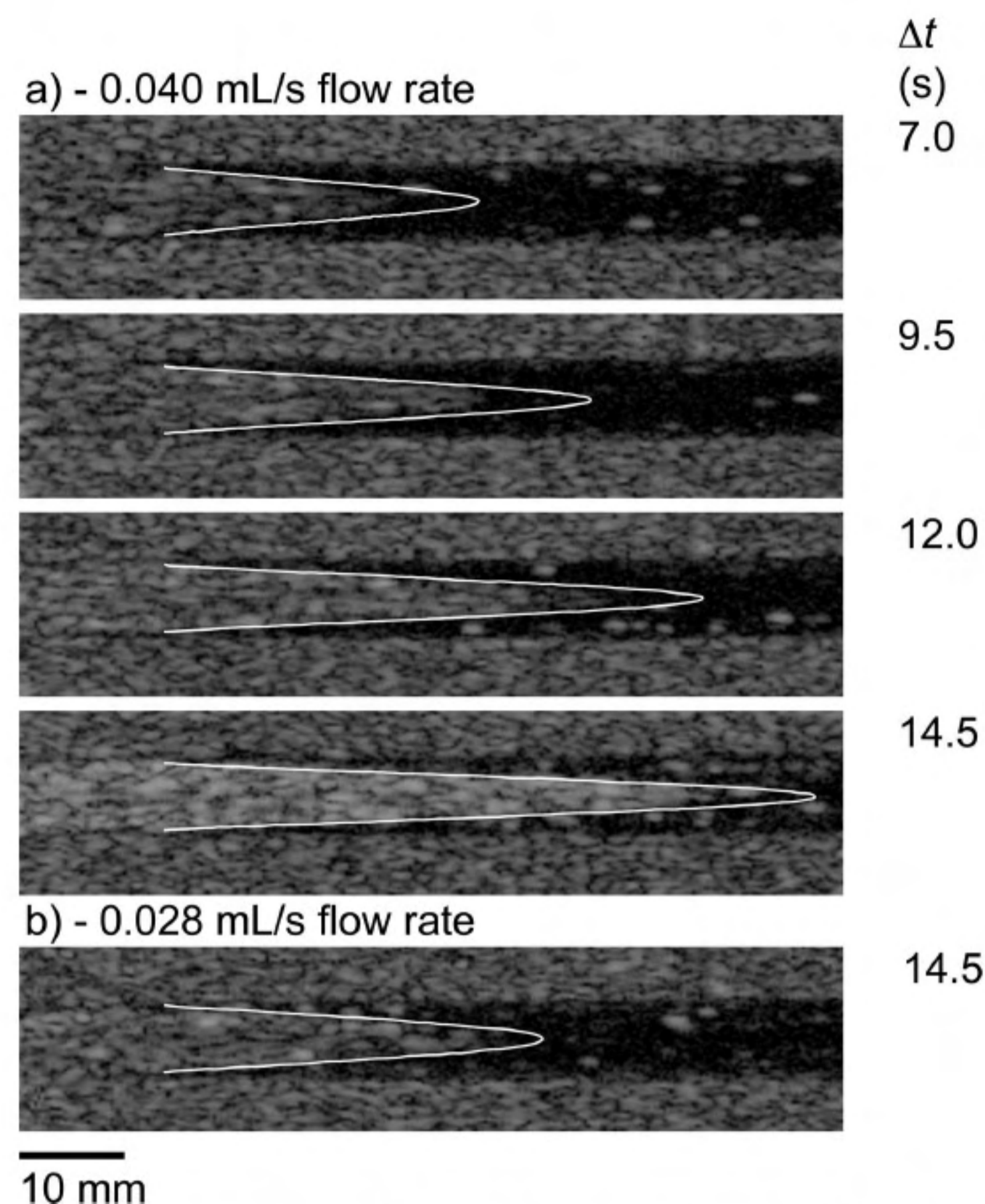


Fig. 7. Reconstructed images along the length of the flow tube, showing the contrast agent flow. These are corrected for the time-dilation effect described in the text and Fig. 1. The white line shows the theoretical position of the contrast front. The flow passed through a tube of radius 3.175 mm at a rate of (a) 0.040 mL/s and (b) 0.028 mL/s. Transducer translation velocity v_T was 6 mm/s. Expected profiles closely match those observed, except at the center of the leading edge. It is believed that the discrepancy is due to slight contrast destruction, due to both increased beam exposure and decreased overlying attenuation from overlying contrast (see text).

tional images with their expected contrast outlines superimposed are shown in Fig. 7 for each sweep, with the flow rate and effective transducer separation noted. Since the transducer translation velocity v_T (6 mm/s throughout) was greater than the maximum flow velocity v_c , the imaging transducer reached and overtook the refilling front for each sweep. At all times, the radius of the observed contrast should be that found by eqn 3. As expected, for the reduced flow rate shown in Fig. 7b, the contrast profile does not progress as far as that for an identical Δt (14.5 s). Examination of the images in Fig. 7 reveals a generally good match between the observed profiles and those predicted, with the clear exception being the axial center of each profile. The center of the profile does not progress as far as the prediction and the discrepancy is greater for higher flow rates. Fitting the measured radii to eqn 4 to estimate v_c gives estimated values shown in Fig. 8 for all scans acquired. The mean measured center velocities were (\pm std dev) 1.46 ± 0.21

and 2.25 ± 0.5 corresponding, respectively, to expected values of 1.75 and 2.50 (all in mm/s). In a statistical comparison with the expected values, a Student's t -test yields $p = 0.07$ and 0.39; as such, the measured velocities cannot be said statistically to differ from those expected, although there may be a trend toward an underestimation.

The slight discrepancy between the expected and observed contrast profiles within the cylindrical tube phantom may be due to some minimal amount of contrast clearance from repeated low-power ultrasound exposure during the imaging process. Contrast clearance is more pronounced near the center of the tube than at the edges, due to the reduction in relative velocities between the flow and the transducer. The reduction in relative velocity causes contrast near the tube center to receive more exposure and, hence, preferentially to clear it relative to other contrast, as modeled in Fig. 9. In addition, the reduction in overlying attenuation at the axial center also contributes to increased contrast clearance. In spite

Fitted v_c Results Based on Measured Contrast Radii

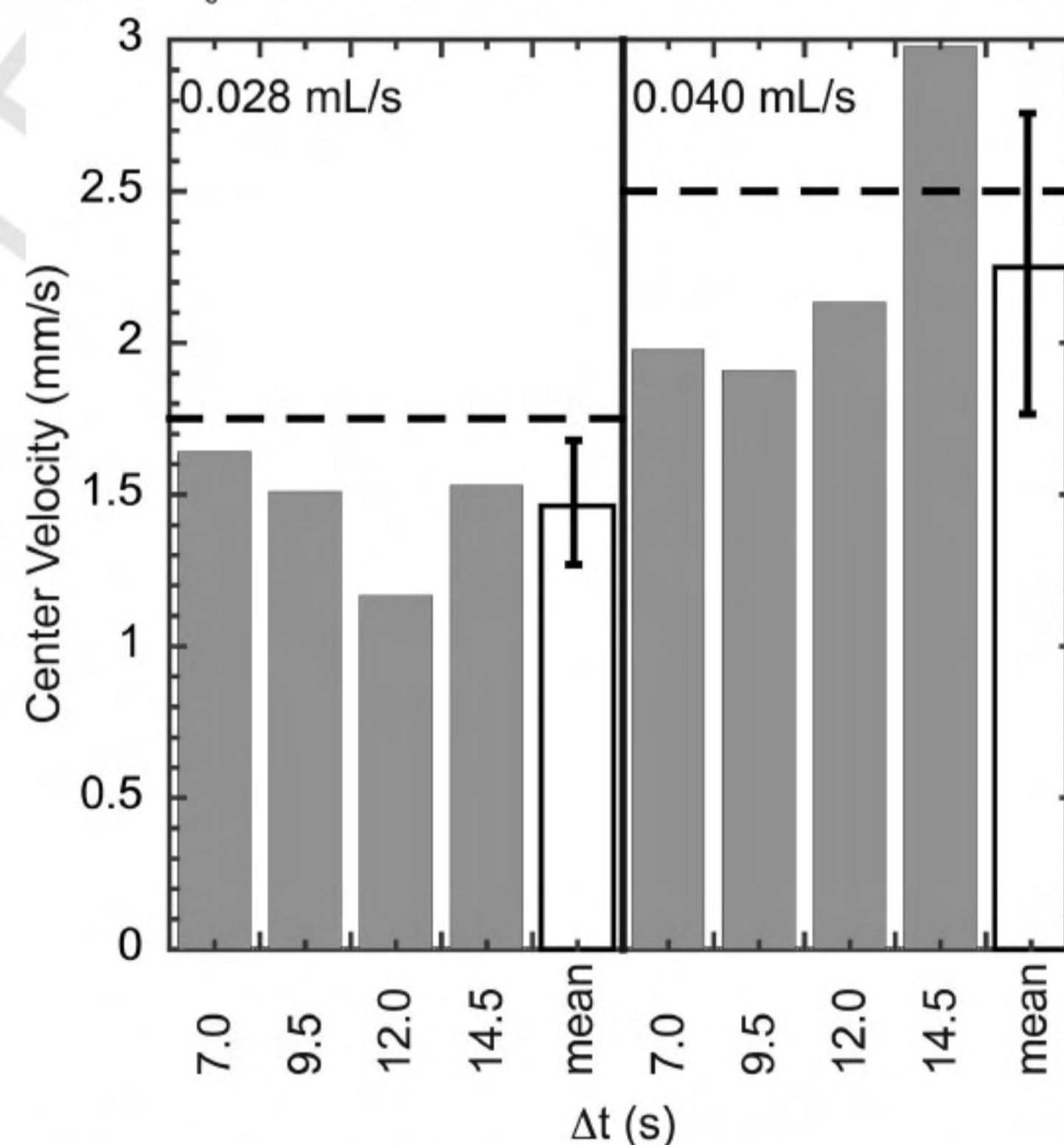


Fig. 8. Fitted v_c results for cylindrical tube phantom. Dual transducer scans were acquired for the cylindrical tube phantom with two center flow velocities (1.75 and 2.50 mm/s, corresponding to the flow rates of 0.028 and 0.040 mL/s, respectively, from Fig. 7) using four different refill times. Shown are the measured values of v_c (1.46 and 2.25 mm/s) obtained by fitting measured contrast radii given in eqn 4 for all measurements along with the mean and standard deviation for the measurements grouped by flow rate. Dashed lines denote theoretically known values of v_c . The measurements tended to be less than those expected, except for one case ($\Delta t = 14.5$ s, 0.040 mL/s flow rate), although the difference in all cases was not statistically significant ($p > 0.05$).

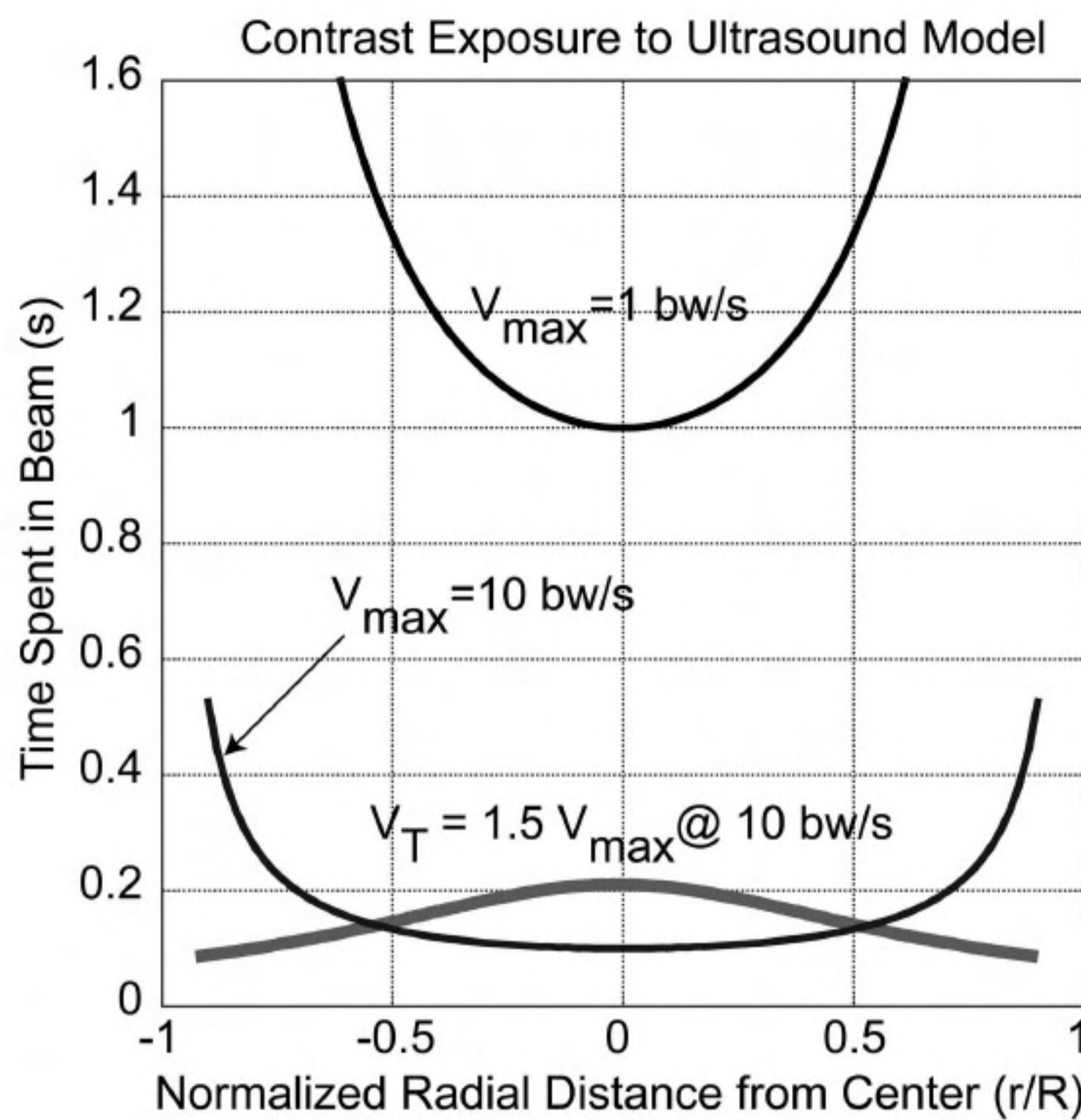


Fig. 9. Simplified model of time spent in the ultrasound beam for various flow speeds. Flow speeds are represented in “beam-widths” per second (bw/s) for normalization. Flow velocity V is considered to be parabolic, with a profile given by $V(r) = V_{\max}[1 - (r/R)^2]$, where r is the tube radius and V_{\max} is the maximum velocity. With a stationary transducer, the fluid closest to the tube wall is exposed to the beam for the longest period of time and these exposure durations decrease with increased flow velocity, as shown by the three curves representing V_{\max} at 1 and 10 bw/s. The thicker shaded curve represents what happens as the transducer is translated along the axis of the tube at a speed higher than the maximum flow velocity. In this case, where V_{\max} was set to 10 bw/s and the transducer speed V_T was set to 1.5 times V_{\max} , the maximum exposure to the beam occurs at the center of the tube. This may help to explain the center peak cutoff of the flow profiles shown in Figure 7. That is, the contrast may be exposed to sufficient pulses in the center to break the bubbles at higher flow velocities. This effect is compounded by the fact that there is also less overlying attenuation, due to the profile shape.

of the effects of slight contrast clearance, peak flow velocity was measured on average to within 13.2% of that expected.

CONCLUSIONS AND DISCUSSION

We have demonstrated the efficacy of a new technique in contrast refill imaging. The dual transducer technique allows the imaging of contrast destruction/refill data in a three-dimensional volume in a drastically reduced time frame, compared with traditional techniques (real-time refill and interval imaging). The tube phantom provided a four-dimensional model that allowed the verification of the dual-transducer technique by comparing expected and observed contrast profiles.

To our knowledge, this model has not previously been employed in four-dimensional imaging. Fitting observed profile radii to those predicted by eqn 4 gave center velocity measurements v_c that tended to be less than those expected, except for one case ($\Delta t = 14.5$ s, 0.040 mL/s flow rate), although the difference in all cases was not statistically significant ($p > 0.05$). The v_c measurements may be low because of slight contrast clearance, which is exhibited in two ways. Looking closely at Fig. 7, one notes, first, that the observed profiles were truncated at their center. Second, the edge of the contrast profile tended to fall on or within ($r \leq r_{\text{expected}}$) the theoretical edge. Radii measurements less than those expected would depress the fitted v_c value.

The exception to the depressed v_c measurements is notable in that the observed contrast profile, as illustrated in Fig. 7, exceeds the theoretical curve ($r > r_{\text{expected}}$) in places and that the profile is notably brighter than the others. The increase in brightness could be due to higher contrast agent concentration for this scan. This scan was the first in the series and the contrast concentration could have been greater than in the other scans due to contrast depletion through the course of the experiment. Without adjusting for this brightness increase, the observed edge for a given threshold would be farther from the center, due to partial volume effects. This increase in the observed radii would then raise the fitted v_c .

Theoretically, radiation force effects could distort the flow of contrast agent through the flow phantom by pushing the contrast away from the tube center. However, radiation force effects were not evident in the observed profiles, since the circular cross-sectional images of the contrast tended to remain centered in the tube throughout, as seen in Fig. 6.

We have shown that the technique gives expected results in the laminar tube flow phantom. The laminar tube flow phantom provided a four-dimensional flow with well-known characteristics, albeit one that is directional. In perfused tissues, the vasculature is much less directional, often having no clear direction of flow visible in the capillary bed. A perfused vascular bed, nevertheless, should be imageable in 3D with this method, using alternative measures of agent flow, such as contrast mean transit time previously mentioned. Further studies will be needed to test this method under in vivo conditions.

Acknowledgments—This project was sponsored by the US Army under grant DAMD17-01 to 1-0327 and grants R01-DK56658 and P01-CA87634 from the US National Institutes of Health (NIH).

REFERENCES

Bell DS, Bamber JC, Eckersley RJ. Segmentation and analysis of colour Doppler images of tumour vasculature. *Ultrasound Med Biol* 1995;21(5):635–647.

AQ:3

- Bhatti PT, LeCarpentier GL, Roubidoux MA, et al. Discrimination of sonographically detected breast masses using frequency shift color Doppler imaging in combination with age and gray scale criteria. *J Ultrasound Med* 2001;20(4):343–350.
- Carson PL, Moskalik AP, Govil A, et al. The 3D and 2D color flow display of breast masses. *Ultrasound Med Biol* 1997;23(6):837–849.
- Carson PL, Fowlkes JB, Roubidoux MA, et al. 3-D color Doppler image quantification of breast masses. *Ultrasound Med Biol* 1998;24(7):945–952.
- Chan CCW, Ng EHY, Li CF, Ho PC. Impaired ovarian blood flow and reduced antral follicle count following laparoscopic salpingectomy for ectopic pregnancy. *Hum Reprod* 2003;18(10):2175–2180.
- Cosgrove DO, Bamber JC, Davey JB, McKinna JA, Sinnett HD. Color Doppler signals from breast tumors. Work in progress. *Radiology* 1990;176(1):175–180.
- Cosgrove DO, Kedar RP, Bamber JC, et al. Breast diseases—Color Doppler US in differential-diagnosis. *Radiology* 1993;189(1):99–104.
- Delorme S, Weisser G, Zuna I, et al. Quantitative characterization of color Doppler images: Reproducibility, accuracy and limitations. *J Clin Ultrasound* 1995;23(9):537–550.
- Folkman J, Beckner K. Angiogenesis Imaging. *Acad Radiol* 2000;7:783–785.
- Hochmuth A, Boehm T, Bitzer C, et al. Differentiation of breast masses using 3-D sonographic and echo-enhancer-based evaluation of the vascular pattern: Initial experiences. *Ultrasound Med Biol* 2002;28(7):845–851.
- Hoskins PR. Ultrasound techniques for measurement of blood flow and tissue motion. *Biorheology* 2002;39(3–4):451–459.
- Jokubkiene L, Sladkevicius P, Rovas L, Valentin L. Assessment of changes in endometrial and subendometrial volume and vascularity during the normal menstrual cycle using three-dimensional power Doppler ultrasound. *Ultrasound Obstet Gynecol* 2006;27:672–679.
- Kamiyama N, Moriyasu F, Kono Y, et al. Investigation of the “flash echo” signal associated with a US contrast agent. *Radiology Suppl S* 1996;201:165.
- Kamiyama N, Moriyasu F, Mine Y, Goto Y. Analysis of flash echo from contrast agent for designing optimal ultrasound diagnostic systems. *Ultrasound Med Biol* 1999;25(3):411–420.
- Kedar RP, Cosgrove DO, Bamber JC, Bell DS. Automated quantification of color Doppler signals: A preliminary study in breast tumors. *Radiology* 1995;197(1):39–43.
- Kedar RP, Cosgrove D, McCready VR, Bamber JC, Carter ER. Microbubble contrast agent for color Doppler US: Effect on breast masses. Work in progress. *Radiology* 1996;198(3):679–686.
- LeCarpentier GL, Chen NG, Fowlkes JB, Carson PL. A New Dual-Transducer Method of Three-Dimensional Ultrasound Contrast Agent Imaging of Vascularity. (proceedings of the 10th Congress of the World Federation for Ultrasound Med Biol) *Ultrasound Med Biol* 2003;29(5S):S53.
- Lee WJ, Chu JS, Huang CS, et al. Breast cancer vascularity: Color Doppler sonography and histopathology study. *Breast Cancer Res Treat* 1996;37(3):291–298.
- Mehta SS, Azzouzi AR, Hamdy FC. Three dimensional ultrasound and prostate cancer. *World J Urol* 2004;22:339–345.
- Merce LT, Barco MJ, Bau S, Kupesic S, Kurjak A. Assessment of placental vascularization by three-dimensional power Doppler “vascular biopsy” in normal pregnancies. *Croat Med J* 2005;46(5):765–771.
- Moskalik A, Carson PL, Rubin JM, et al. Analysis of three-dimensional ultrasound Doppler for the detection of prostate cancer. *Urology* 2001;57(6):1128–1132.
- Moskalik AP, Rubin MA, Wojno KJ, et al. Analysis of three-dimensional Doppler ultrasonographic quantitative measures for the discrimination of prostate cancer. *J Ultrasound Med* 2001;20(7):713–22.
- Ohmori K, Cotter B, Kwan OL, Mizushige K, DeMaria A. Relation of contrast echo intensity and flow velocity to the amplification of contrast opacification produced by intermittent ultrasound transmission. *Am Heart J* 1997;134:1066–1074.

- Peters-Engl C, Medl M, Mirau M, et al. A Color-coded and spectral Doppler flow in breast carcinomas-relationship with the tumor microvasculature. *Breast Cancer Res Treat* 1998;47(1):83–89.
- Porter T, Xie F. Transient myocardial contrast after initial exposure to diagnostic ultrasound pressures with minute doses of intravenously injected microbubbles. Demonstration and potential mechanisms. *Circulation* 1995;92(9):2391–2395.
- Porter TR, Li S, Kricsfeld D, Armbruster RW. Detection of myocardial perfusion in multiple echocardiographic windows with one intravenous injection of microbubbles using transient response second harmonic imaging. *J Am Coll Cardiol* 1997;29(4):791–799.
- Porter TR, Li S, Jiang L, Grayburn P, Deligonul U. Real-time visualization of myocardial perfusion and wall thickening in humans with intravenous ultrasound contrast and accelerated intermittent harmonic imaging. *J Am Soc Echocardiogr* 1999;12:266–271.
- Potdevin TC, Moskalik AP, Fowlkes JB, Bude RO, Carson PL. Doppler quantitative measures by region to discriminate prostate cancer. *Ultrasound Med Biol* 2001;27(10):1305–1310.
- Simpson DH, Chin CT, Burns PN. Pulse inversion Doppler: A new method for detecting nonlinear echoes from microbubble contrast agents. *IEEE Ultrason Ferroelectr Freq Control* 1999;46(2):372–382.
- Vaupel P, Kallinowski F, Okunieff P. Blood flow, oxygen and nutrient supply, and metabolic microenvironments of human tumors: A review. *Cancer Research* 1989;49:6449–6465.
- Wei K, Jayaweera AR, Firoozan S, et al. Quantification of myocardial blood flow with ultrasound-induced destruction of microbubbles administered as a constant venous infusion. *Circulation* 1998;97(5):473–483.
- Weidner N, Semple JP, Welch R, Folkman J. Tumor angiogenesis and metastasis correlation in invasive breast carcinoma. *N Engl J Med* 1991;324:1–8.

APPENDIX

The required scan times for imaging a three-dimensional volume using interval imaging, real-time refill and the dual-beam technique (demonstrated here with two transducers) are calculated as follows:

ρ : slice density (slices/unit length)

T: volume thickness (length units)

N_s : number of slices, $N_s = \rho T$

N_t : number of time points

t_{clear} : contrast clearance time needed for one slice

t_{max} : maximum time point acquired on refill curve

v_T : transducer translation speed (distance/unit time), $v_T = N_t t_{trans}$

(see below)

t_{trans} : time to translate one slice thickness, $t_{trans} = 1/(\rho v_T)$,

$t_{trans} \rightarrow 0$ for two dimensional arrays where translation is unnecessary to image the volume and imaging rates are controlled by propagation and other processing considerations.

t_M : time to reach time point M, $t_M \leq t_{max}$

t_r : time to return transducers to starting position.

For real-time imaging with a one-dimensional array, the time required is

$$N_s[t_{clear} + t_{max} + t_{trans}], \quad (5)$$

which is the number of slices N_s multiplied by the time required to acquire one slice (time to clear the plane plus the maximum time point in the refill curve), plus the time needed to translate the transducer one slice thickness. The number of time points acquired is limited only by the transducer frame rate and does not affect the acquisition time.

For interval imaging, the time required is

$$N_s \left[\sum_{M=1}^{N_t} (t_{clear} + t_M) + t_{trans} \right], \quad (6)$$

where $t_M \leq t_{max}$ and the sum is the total time required to obtain the image for all time points t_M . The required time can vary, significantly, depending on the selection of points t_M .

The time required for the scans using two transducers to demonstrate the dual beam technique is given by

$$\sum_{M=1}^{N_t} [N_s t_{trans} + t_M + t_r] - t_r, \quad (7)$$

where the clearance transducer has traversed the volume in $N_s t_{trans}$ and the imaging transducer arrives at the volume boundary after time t_M . As N_s is moved into the summation, one can understand how a dramatic reduction in required scan time generally takes place compared with conventional real-time and interval acquisition. If imaging and clearance could be alternated between the two transducers, there is no need to return the transducers to their starting position after each sweep. Under such circumstances, t_r would be 0.

Note that the time required with the dual transducer technique does not depend on the number of slices acquired for a given v_T . That

is, for a given v_T , an increase in the number of slices N_s would result in a corresponding decreases in the translation time between slices t_{trans} and overall acquisition time would remain constant. The velocity v_T is generally constrained by the acoustic frame rate (AFR) and desired slice density ρ , *i.e.*, $v_T \leq \text{AFR}/\rho$, rather than by the capabilities of the translation system. The minimum t_M that can be acquired is limited by translation velocity v_T and the minimum transducer separation. Clearance time t_{clear} is not present, because the clearance transducer clears the volume as it is swept.

For a 2D array imaging, a volume completely contained within its field-of-view, the scan time required is given by eqns 5 and 6 for real-time and interval imaging, respectively, (with $N = 1$). The term $t_{trans} \rightarrow 0$ and the imaging rate is limited by the volumetric frame rate and beam propagation considerations. The minimum acquirable t_M is based on the time required electronically to sweep through and read the volume.

UNCORRECTED PROOF

Rapid 3D Imaging of Contrast Flow II: Application to Perfused Kidney Vasculature

Chen NG†, Fowlkes JB†‡, Carson PL†‡, LeCarpentier GL‡

Departments of Biomedical Engineering†/Radiology‡, University of Michigan, Ann Arbor, MI, USA

Please send all correspondence to:

Gerald L LeCarpentier, PhD

University of Michigan Dept of Radiology

Basic Radiological Sciences

200 Zina Pitcher Place Rm 3315

Ann Arbor, MI 48109-0553

(734) 647-9326 (Telephone)

(734) 764-8541 (FAX)

gllec@umich.edu

3D Imaging of Contrast Flow II

Rapid 3D Imaging of Contrast Flow II: Application to Perfused Kidney Vasculature

Abstract

As noted in Part I of this study, refill imaging of ultrasound contrast in a 3D volume is potentially superior to 2D imaging for vascular characterization. A dual plane, dynamic refill technique was used to image a preserved porcine kidney perfused with contrast. For a $4.7 \times 5 \times 9 \text{ cm}^3$ volume, high-speed 3D refill imaging for 7 time-point measurements up to 288 seconds was effective with an imaging time reduction of 96% over corresponding real-time imaging. Mean transit times (MTTs) were estimated for regions of interest (ROIs) within renal cortex in both cross-sectional and longitudinal planes extracted from reconstructed volumes. MTTs for these ROIs were also obtained using conventional means for comparison. After correcting for contrast degradation over time, dual beam measurements were statistically equivalent to those conventionally obtained. These experiments demonstrate that this dual beam technique effectively images 3D contrast refill in greatly reduced time.

Keywords: contrast refill, perfusion, blood flow, imaging, vasculature, angiogenesis, time-intensity curve

Introduction

Refill imaging of ultrasound contrast agent perfusion in a three-dimensional volume may allow superior vascular characterization of tissues when compared to two-dimensional imaging (Carson et al. 1999). Visualization and mapping of the blood flow within and surrounding tumors may provide a means for differentiating between benign and malignant masses (Bhatti et al. 2001; LeCarpentier et al. 1999). After contrast is cleared from a volume, its refill can be monitored. For any given region of interest, signal intensities can be plotted as a function of refill time and fitted to a time-intensity curve from which the contrast mean transit time (MTT) can be estimated.

As previously described in part I (Chen et al. 2005), both traditional real-time refill imaging and interval imaging of contrast refill are impractical in three-dimensions since each slice plane has to be separately acquired for the duration of the refill. The number of slices needed to constitute a three-dimensional volume is significant, and the net acquisition time is the product of that number and the time needed to acquire a single slice. This dependence would lead to excessive scan time requirements, during which the volume would need to be perfused with contrast agent.

The dual-transducer technique illustrated in part I (Chen et al. 2005) is one dual-beam method for collection of three-dimensional data. Sweeping a transducer pair, composed of a clearance transducer and a low-power imaging transducer as a unit at velocity v over a contrast perfused tissue volume collects the refill images of the entire volume at a refill time. Slice separation is determined by both the trigger rate of the imaging transducer and the translation velocity v as described in the appendix of part I (Chen et al. 2005) and has a minimal effect on acquisition time.

In order to test the effectiveness of a dual-beam method in imaging a perfused vascular bed, a preserved porcine kidney is used as a three-dimensional phantom (Holmes et al. 1984). Such a phantom contains a vascular bed and provides an environment to test the dual transducer technique with a more realistic spatial distribution of flow than the cylindrical tube phantom previously reported (Chen et al. 2005). Comparison of MTTs obtained in dual transducer acquisitions with those using real-time (Porter et al. 1999; Simpson et al. 1998) and interval imaging (Kamiyama et al. 1996; Moriyasu et al. 1996; Ohmori et al. 1997; Wei et al. 1998) can be used to demonstrate the efficacy of a dual-beam method. Validation of the three-dimensional nature of the acquisition is performed by examining the images in the lateral-elevational plane of the dual transducer acquisitions and comparing those images to corresponding images directly acquired.

Theoretical Considerations

In a perfused vascular bed, contrast agent fills the blood vessels, and it is assumed that the agent follows the fluid flow perfusing the bed. Immediately after contrast clearance and the cessation of the high-powered insonation, contrast from outside the disruption zone begins to refill the cleared volume. The refill can be measured either continuously with low-power pulses (real-time refill imaging) or intermittently at only specified times. Alternatively, the refill can be imaged at high power at specified intervals, the contrast being cleared after each acquisition for the next time point to be measured (interval imaging). The contrast signal intensity (assumed proportional to the contrast concentration) at the measured time points can then be fitted to an exponential equation of the form $y(t) = A[1 - \exp(-t/MTT)]$, where A is the

signal value at the asymptotic limit, t the time interval, and MTT the mean transit time (Wei et al. 1998). Differing flow dynamics would result in different MTT values, while the value of A depends on the contrast agent and its tissue concentration, and is assumed independent of the flow itself.

Experimental Methods

Ultrasound scans were conducted within a tank lined with sound absorbent rubber and filled with water that had been allowed to come to gas saturation. A schematic of the experimental setup is shown in Figure 1. The kidney (preserved as described below) was mounted beneath the water on a stand and secured with two rubber bands. As previously described in part I (Chen et al. 2005), a dual transducer assembly was used to demonstrate the dual beam technique by controlling both transducer separation and translation along the transducers' elevational direction. The transducer assembly was mounted upon a second stand that placed the transducers above the kidney being scanned.

A porcine kidney was obtained and preserved (Holmes et al. 1984) and subsequently rehydrated and degassed by perfusion through the renal artery with (> 5 L) degassed water. The kidney was subsequently perfused with a 1:5000 Definity/water suspension at 33 mL/min using a peristaltic pump (Cole-Parmer L/S pump and drive, Cole-Parmer Instrument Corporation, Barrington, IL, USA). Dual transducer scans in the transverse orientation as shown in Figure 2 were made with the Toshiba Powervision (Toshiba Corporation, Otawara-shi, Tochigi-Ken, Japan) system using the PVN-375AT transducer for contrast clearance. In order to consistently adjust power output and firing

rate, the transducer was placed in harmonic mode (power setting of P8 at a frame rate of 10 Hz). The GE Logiq 9 (General Electric Corporation, Milwaukee, WI, USA) 7L transducer in phase inversion (PI) mode at low power (2% acoustic output-AO) was the imaging transducer. Images for a 90 mm thick volume of interest for refill times of 16, 32, 48, 96, 144, 288, and 432 sec with a 1 mm slice separation were acquired. The GE Logiq 9 was specifically adapted to store triggered images into the cine buffer through the opening and closing of its footswitch control. As the transducer was translated, slice separation was controlled by opening and closing the control with a solid-state relay (manufacturer and model) with a LabVIEW (National Instruments Corporation, Austin, TX, USA) script. For the translation speed of 6 mm/sec, a triggering rate of 6 Hz provided the 1 mm slice separation in the acquisitions. In addition, a set of sparsely acquired dual-transducer images were taken with a slice separation of 20 mm in order to demonstrate the independence of the refill behavior from the slice spacing.

Refill data using real-time and interval imaging methods were collected using the GE L9 at a single slice position in the transverse orientation for comparison with dual transducer results. Using the footswitch trigger, fifty clearance pulses at 5 Hz were fired at high power (100% AO), and images subsequently collected at 2% AO at a 1 Hz frame rate for real-time refill. Interval imaging was performed using the same clearance pulse sequence, and imaging of contrast signal for different intervals at both 2% and 100% AO. The measured signal intensities for the kidney perfused with water (no contrast) were then subtracted from those of the other images, and fitted to the exponential equation $f(t)=A[1-\exp(-t/MTT)]$ for a region of interest in the kidney cortex and compared among the different methods.

A slice in the longitudinal direction was imaged using interval imaging and real-time refill for comparison with a longitudinal image plane extracted from the 3D volume acquired with the dual transducer technique to demonstrate its 3D capabilities. The extracted images in the longitudinal orientation corresponding to those directly acquired were selected using image registration with MIAMI Fuse software developed at the University of Michigan (Meyer et al. 1997; Meyer et al. 1999). Mean transit times for a region of interest were recorded for each technique and compared.

Results

Representative images indicated in Figure 3 show a selected transverse slice (i.e. with slice orientation as those acquired by the dual transducer (DT) method) imaged using both interval imaging (II) and real-time refill (RT) compared with corresponding DT images. Figure 4 shows some representative refill curves corresponding to the images. In Figure 5A, the estimated MTT values are compared for data acquired using each method, and the values follow a clear trend. Dual transducer measurements were shorter than those otherwise measured but were consistent with each other. The MTT for the DT sparse case is comparable to the other DT MTT measurements, indicating that slice spacing did not affect the DT measurement results. The MTT for the II sequence taken at 100% AO had a shorter MTT than that taken at 2% AO, and both were shorter than those acquired using RT.

The elevation in MTTs measured through real-time refill relative to data obtained otherwise was possibly due to a slight decrease in overall contrast signal level over the course of each experiment. Such a decay in contrast signal would cause a decrease in

MTT measured with II at 2% AO, which requires a relatively long time to acquire and would otherwise be expected to match the RT measured value. Contrast degradation is minimal for RT acquisitions since any time point being measured requires only the elapsed time from the end of the contrast clearance sequence. For example, the time point of 288 sec requires only 288 sec of elapsed time. On the other hand, for the II case where the time points were acquired sequentially, the same 288 sec (4.8 min) time point would be acquired 714 sec (11.9 min) after initial contrast clearance at the start of the experiment since there was acquisition time associated with all the other time points measured. The DT scans require similar times as II; however it should be noted that the refill imaging for the entire volume is performed during that time, as opposed to a single slice plane acquisition in the case of RT and II.

Contrast degradation over time can be modeled as a decaying exponential of the form $y(t)=Ae^{-\beta t}$, with a constant β , which corresponds to a fixed percentage of contrast signal per unit time. A slight decrease in contrast signal over time would skew the MTT curve fit by artificially depressing the latter data points as shown in Figure 6A. Further evidence for a slight decrease in signal level over time is found in the signal level ratios shown in Table 1. The ratios are approximately identical at short times, but they diverge at longer time points. Since the longer time points for II and DT are acquired at times significantly longer than those of RT post-infusion, slight contrast degradation with time would be consistent with this divergence in ratios.

One can compensate for the contrast decay by normalizing the measured signal intensities by $e^{-\beta t}$ for the times t at which the images were collected. Since the refill dynamics for the RT measurements and their corresponding II taken at an acoustic

output of 2% are identical, the measured MTTs should be statistically identical. The difference in their directly measured values can be ascribed to the contrast decay and used to estimate the contrast decay over time by determining the correction factor that would statistically equalize the MTTs. It was found that a correction factor of 4.1% per minute applied to both the RT and II measurements would cause the mean RT MTT to fall within the 95% confidence interval of the II measurement. Correction factors for the other acquisitions that would equalize the measured MTTs to statistical significance are indicated in Figure 5B.

Dual transducer images were assembled to form three-dimensional images of the kidney for each acquisition time point. Representative reconstructed slices corresponding to those directly acquired perpendicular to the dual-transducer images, as well as those directly acquired images, are shown in Figure 7. For the marked ROI, the measured MTTs for each technique follow the trend for the transverse case, and can likewise be corrected to approximately equal values as shown in Figure 8. The successful image reconstruction and MTT correspondence with directly acquired data demonstrate the ability of the DT technique to generate true 3D refill data.

Conclusions and Discussion

We have demonstrated the efficacy of a new technique in contrast refill imaging. The dual transducer technique allows the imaging of contrast destruction/refill data in a three-dimensional volume in a drastically reduced time frame, compared to traditional techniques (real-time refill and interval imaging). The ability of the dual transducer technique to obtain mean transit time (MTT) measurements similar to those of

conventional methods but in a fraction of the time, and to generate meaningful longitudinal images perpendicular to the scan direction suggests this technique is useful in imaging the vasculature of perfused tissue on a three-dimensional basis.

Due to the restrictions on contrast flow rate associated with the perfused kidney phantom used here, contrast decay unfortunately plays an important role in skewing measured MTTs. However in clinical practice contrast decay effects would be negligible *in vivo* where the MTTs measured are typically much shorter (such as those from Seidel et al. 1999) the effect of which is shown in Figure 6B. In addition, if necessary, any decay could be readily corrected by monitoring the decay via a major vessel. Nevertheless, the dual transducer measurements were consistent with each other without correction, and at the very least provided a measure of relative MTT.

Correction factors that would statistically equalize (as previously described) the RT measured MTTs with the DT scans and II at 100% AO scan were also computed and are indicated in Figures 5B and 8B. However, the DT and II MTTs may *indeed* differ from RT MTTs due to differing flow dynamics. The DT technique clears the entire volume of interest of contrast before imaging the refill as opposed to RT, where only a single slice plane is cleared prior to imaging. In II at 100% AO, there is the same contrast clearance pattern as RT; however, the slice thickness of the imaging plane may be broader due to the increased acoustic output used, causing contrast to refill the imaging plane sooner and reducing MTT. These differences, which are not accounted for here, could affect measured MTTs in addition to contrast degradation.

Image quality of the longitudinal images obtained using the dual transducer technique is limited only by the acquisition frame rate and the transducer elevational

point-spread function. Our previous work with this transducer (unpublished observations) suggests that longitudinal image quality is not appreciably improved at a slice separation below $\sim 500\text{ }\mu\text{m}$, which can be readily achieved with the dual transducer technique with no increase in scan time requirements.

We have shown previously that the technique gives expected results in a laminar tube flow (Chen et al. 2005) and now in a preserved kidney phantom. The DT technique is only one of several possible dual beam methods that could be used to image a three-dimensional volume. With a two-dimensional array, mechanical translation can become unnecessary and acquisition times reduced from those needed by the DT technique demonstrated here. The dual-beam techniques can readily be applied toward living tissues with their higher flow rates and hence shorter MTTs, thereby avoiding all contrast degradation issues, to produce a practical means of obtaining three-dimensional contrast perfusion images.

Acknowledgement

This project was sponsored by the US Army under grant DAMD17-01-1-0327 and R01-DK56658 from the US National Institutes of Health (NIH). Kimberly Ives, DVM kindly assisted in the acquisition and preparation of the porcine kidney. Dr. Huzefa Neemuchwala kindly assisted in providing scripts used in preserving proper image aspect ratios, and Sakina Zabuawala assisted in the use of MIAMI Fuse.

References

- Bhatti PT, LeCarpentier GL, Roubidoux MA, et al. Discrimination of Sonographic Breast Lesions Using Frequency Shift Color Doppler Imaging, Age and Gray Scale Criteria. *J Ultrasound Med* 2001; 20:343-350.
- Carson PL, Moskalik AP, Govil A, et al. The 3D and 2D Color Flow Display of Breast Masses, *Ultrasound Med Biol* 1997; 23(6) 837-849.
- Chen NG, Fowlkes JB, Carson PL, LeCarpentier GL. High Speed 3D Imaging of Ultrasound Contrast Flow Dynamics Part I: Demonstration of a dual Beam Technique. *Ultrasound Med Biol* 2005 (submitted).
- Holmes KR, Ryan W, Weinstein P, Chen MM. A fixation technique for organs to be used as perfused tissue phantoms in bioheat transfer studies. *ASME ADV BIOENG*, 1984; 9-10.
- Kamiyama N, Moriyasu F, Kono Y, et al. Investigation of the “flash echo” signal associated with a US contrast agent. *Radiology* 1996; 201(165).
- LeCarpentier GL, Bhatti PT, Fowlkes JB, et al. Utility of 3D Ultrasound in the discrimination and detection of breast cancer. *RSNA EJ*, 1999; <http://ej.rsna.org/ej3/0103-99.fin/titlepage.html>.
- Meyer CR, Boes JL, Kim B, et al. Demonstration of accuracy and clinical versatility of mutual information for automatic multimodality image fusion using affine and thin plate spline warped geometric deformations. *Med Image Anal* 1997; 1(3) 195-206.
- Meyer CR, Boes JL, Kim B, et al. Semiautomatic Registration of Volumetric Ultrasound Scans. *Ultrasound Med Biol* 1999; 25(3): 339-347.

Moriyasu F, Kono Y, Nada T, et al. Flash echo (passive cavitation) imaging of the liver by using US contrast agents and intermittent scanning sequence. *Radiology* 1996; 201(374).

Ohmori K, Cotter B, Kwan OL, Mizushige K, DeMaria A. Relation of contrast echo intensity and flow velocity to the amplification of contrast opacification produced by intermittent ultrasound transmission. *Am Heart J* 1997; 134: 1066-1074.

Porter TR, Li S, Jiang L, Grayburn P, Deligonul U. Real time visualization of myocardial perfusion and wall thickening in humans with intravenous ultrasound contrast and accelerated intermittent harmonic imaging. *J Am Soc Echocardiogr* 1999; 12: 266-71.

Seidel G, Greis C, Sonne J, Kaps M. Harmonic grey scale imaging of the human brain. *J Neuroimaging* 1999; 9(3): 171-174.

Simpson DH, Burns PN. Perfusion imaging with pulse inversion Doppler and microbubble contrast agents: in vivo studies of the myocardium. *IEEE Ultrason Symposium* 1998; 2: 1783-1786.

Wei K, Jayaweera AR, Firoozan S, et al. Quantification of Myocardial Blood Flow With Ultrasound-Induced Destruction of Microbubbles Administered as a Constant Venous Infusion. *Circulation* 1998; 97(5): 473-483.

Time (sec)	Real-time		Interval Imaging (2% AO)		Dual-Transducer	
	R _{sig}	t _{acq} (sec)	R _{sig}	t _{acq} (sec)	R _{sig}	t _{acq} (sec)
16 (ref)	1	16	1	31	1	60
32	2.00	32	2.06	78	2.13	180
48	3.47	48	3.33	141	2.80	300
96	6.59	96	5.20	252	4.49	480
144	8.60	144	6.64	411	4.56	720
288	12.97	288	7.90	714	4.42	1140

Table 1 - Ratio of measured signal intensity relative to reference time point at 16 sec.

The ratios are approximately equal for all methods for short intervals, yet diverge with longer time intervals. This divergence is most pronounced for dual transducer data since the DT technique requires the most time, although it is also significant for the interval imaging case. The signal reduction only at longer time points is consistent with a gradual loss of contrast signal strength that would explain the systematic reduction in measured MTT using the II and DT techniques. For actual studies *in vivo*, time-dependent contrast degradation would not be significant because the necessary measurement times would be much shorter (see discussion).

Figure 1 - Schematic of dual-transducer apparatus and experimental setup. The dual-transducer apparatus (modified from the apparatus previously reported) consists of a dual-transducer positioning stage, which consists of translation (M_T) and separation (M_S) motors. Each motor turns a threaded rod, which translates a platform that contains a transducer holder. The platforms translate within the tracked slide. Motors are connected to a powered control module, which contain the electronics driving the motors. The control module is linked to a laptop computer through the DAQCard-700. The control module also contains circuitry needed to operate the footswitch trigger and is linked to the GE (General Electric Corporation, Milwaukee, WI, USA) Logiq 9 footswitch control in order to trigger image acquisition. Using LabVIEW scripts, the imaging transducer (T_i) is triggered and transducers translated as required. The transducers are positioned above the phantom being scanned, with the clearance transducer (T_c) positioned at the edge of the volume of interest. The phantom is continuously perfused with dilute (1:5000 concentration) contrast pumped from a stirred flask.

Figure 2 - Kidney phantom with transducer orientations. The kidney phantom is perfused through the renal artery that is connected to a pump. All dual transducer scans are acquired by translating the transducers as indicated by the arrows, with the transducers oriented in the transverse orientation. For comparison with reconstructed images acquired with the dual transducer technique, the imaging transducer was oriented in the longitudinal orientation perpendicular to the transverse orientation as shown.

Figure 3 - Representative transverse images obtained for a representative slice from preserved porcine kidney with interval imaging, real-time refill, and the dual transducer technique for refill times of 0, 16, and 288 sec. Images from real-time refill and dual transducer are obtained with the same acoustic settings as the 2% acoustic output interval imaging data. Interval imaging images obtained at 100% acoustic output are brighter because of the high transducer output used to obtain the images. Contrast clearance was obtained for both interval imaging cases and real-time refill using 50 pulses at 5 Hz at an acoustic output of 100%. The separate clearance transducer provided contrast clearance for the dual-transducer measurements. A rectangular window marks the region of interest in subsequent mean transit time comparisons.

Figure 4 - Example of measured refill curves. Abbreviations used are as follows: II - Interval Imaging, RT - Real-Time refill, DT - Dual Transducer technique, MTT - Mean Transit Time. Real-time refill imaging provides nearly continuous data for the ROI. Interval imaging and the dual transducer technique provide measurements at specific time points only; however, with a judicious selection of measured points, the MTT can be estimated. The II acquisition was obtained at an acoustic output of 2%. An image was obtained for the II case at 432 sec; however, its corresponding point (255) was excluded because including it would dramatically increase the sum of the squares of the errors (480 vs. 15054). Therefore, the data point was considered an outlier. Fitted MTT results (in sec) for these curves are RT - 182.23, II - 101.44, and DT - 44.55. The earlier

saturation and subsequent signal drop of the II and DT cases are probably due to contrast degradation over time.

Figure 5 - (A) Comparison of data obtained for a given transverse slice, with the ROI (regions of interest) indicated in Figure 8. Numerals refer to repeated acquisitions using the stated method (e.g. DT 3 - third acquired dual transducer data set). Error bars indicate the 95% confidence interval of the mean transit time value, as fitted to the expression $A[1-\exp(-1/MTT)]$ for measured data points. Percentages (for II) refer to the acoustic output (AO) used for readout after set of clearance pulses. Sparse refers to the acquisition where images were obtained at a large (20 mm) slice separation. DT measurements, although differing in absolute terms from corresponding measurements otherwise made, provide a consistent metric of MTT. (B) Factoring in the degradation of contrast agent signal with time, the MTTs can be corrected to values within statistical significance. Because the imaging and flow dynamics are identical for the RT measurements and the II measurement at 2% AO, the MTT should be identical for the measurements. Correcting the RT and II measurements with a contrast degradation factor of 4.1 percent per minute would make the II MTT value statistically equal to the mean of the RT measurements. Applying correction factors (in percent per minute) for the other measurements as indicated would cause the RT MTT mean to be within their 95% confidence interval.

Figure 6 - Effect of contrast decay. If contrast has a rate of decay proportional to the amount present, then its signal intensity would decrease exponentially with time. The

effect on measured MTTs however would only become apparent for experiments requiring relatively long acquisition times. The contrast signal reductions caused by this decay results in the apparent decrease in MTT. (A) Shown are the expected curves for refill dynamics that, with no decay, would result in a 150 sec MTT. Due to the time required to acquire the data set through interval imaging (the time points 16, 32, 48, 96, 144, 288, and 432 sec being acquired at 31, 78, 141, 252, 411, 714, and 1161 sec respectively after beginning acquisition), the observed results are significantly skewed, and without correction would produce a 75 sec MTT. DT acquisitions would also be affected due to their relatively long duration. (B) Contrast decay for short durations. For shorter experimental times, signal decay effects are barely noticeable, as signal level changes are primarily due to contrast fill. Shown here are an ideal refill curve with a 10 sec MTT, measured out to 30 sec and the corresponding II data for a 3%/min decay rate measured at 10, 20, and 30 sec time points for a total acquisition time of 60 sec. In contrast to the previous dramatic skewing of measured MTT, the measured MTT for the II measurement is 9.4 sec. Contrast decay is only significant in longer experimental acquisitions, and would likely be negligible *in vivo*, where experimental duration is significantly shorter.

Figure 7 - Representative longitudinal kidney images analogous to those in Figure 3. The kidney was rotated 90° and had interval refill data (at 100% and 2% acoustic output) and real-time refill measurements taken for the slice plane shown. Refill images for 0, 16, and 288 sec are displayed, with the ROI marked by a rectangular window. Contrast clearance was achieved with 50 100% AO pulses at 5 Hz. The dual transducer

images were obtained by stacking the transverse images from the dual-transducer scans in the elevational direction, and selecting the plane closest to that seen with the perpendicular scans through image registration with the MIAMI Fuse software. The images obtained are of a lower quality because of both the slice separation of 1 mm, and the transducer point-spread function in the elevational direction. However, one still observes contrast filling with time. The marked ROI is that which corresponds closest to the ROI marked in the directly acquired perpendicular images.

Figure 8 - (A) Comparison of mean transit time (MTT) data for perpendicular kidney images with the ROI as indicated in Figure 7. Recon refers to the images formed from the transverse dual transducer scans. MTT trends are identical to those in Figure 5 for analogous reasons. Dual transducer data was consistent among the three acquisitions. Error bars refer to the 95% confidence interval of the curve fit MTT. (B) Results obtained after applying a correction factor analogous to that in Figure 10B. Applying a correction for degradation of 5.3%/min makes the II curve acquired at 2% AO statistically equal to the mean of the corresponding RT measurements. The other measurements require correction factors as indicated to yield MTTs equal to the mean of the RT measurements.

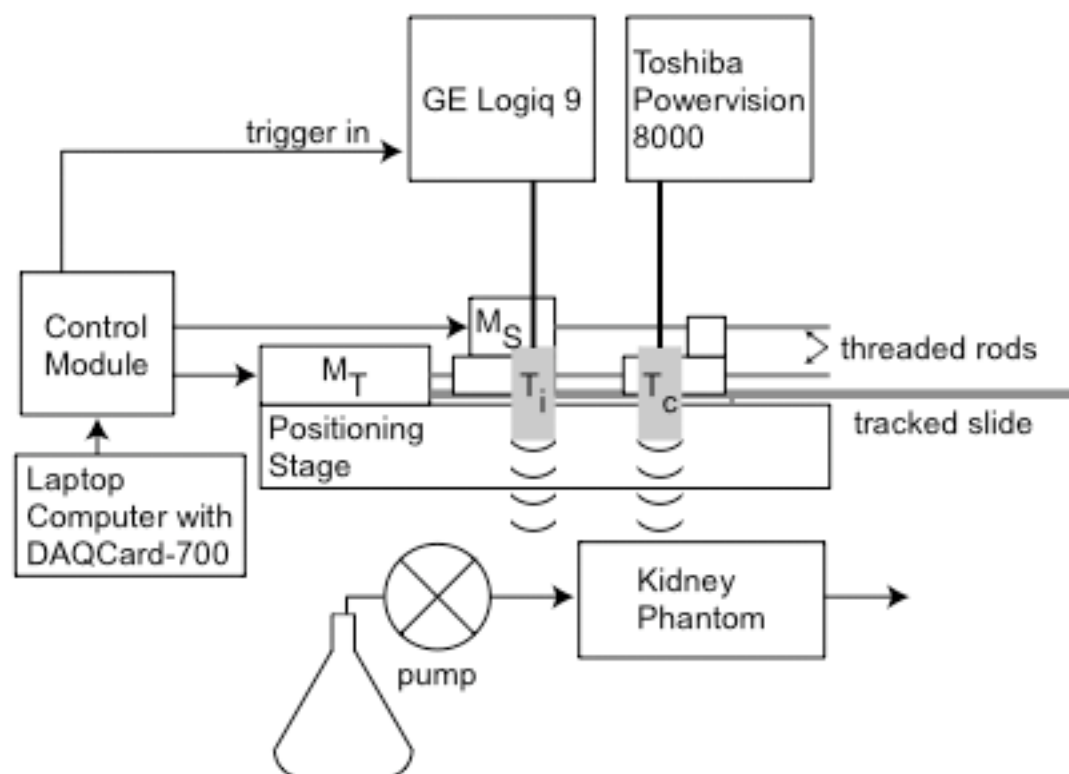


Fig. 1.

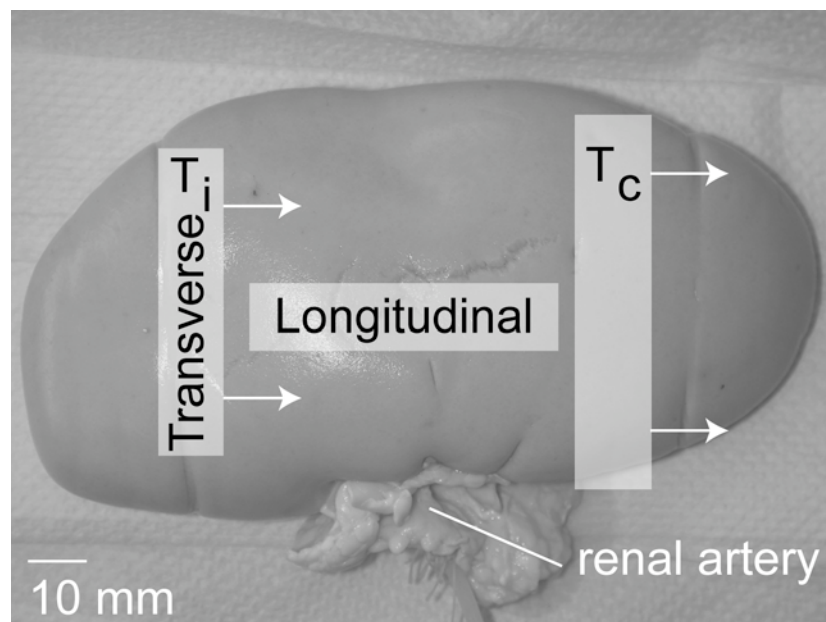


Fig. 2.

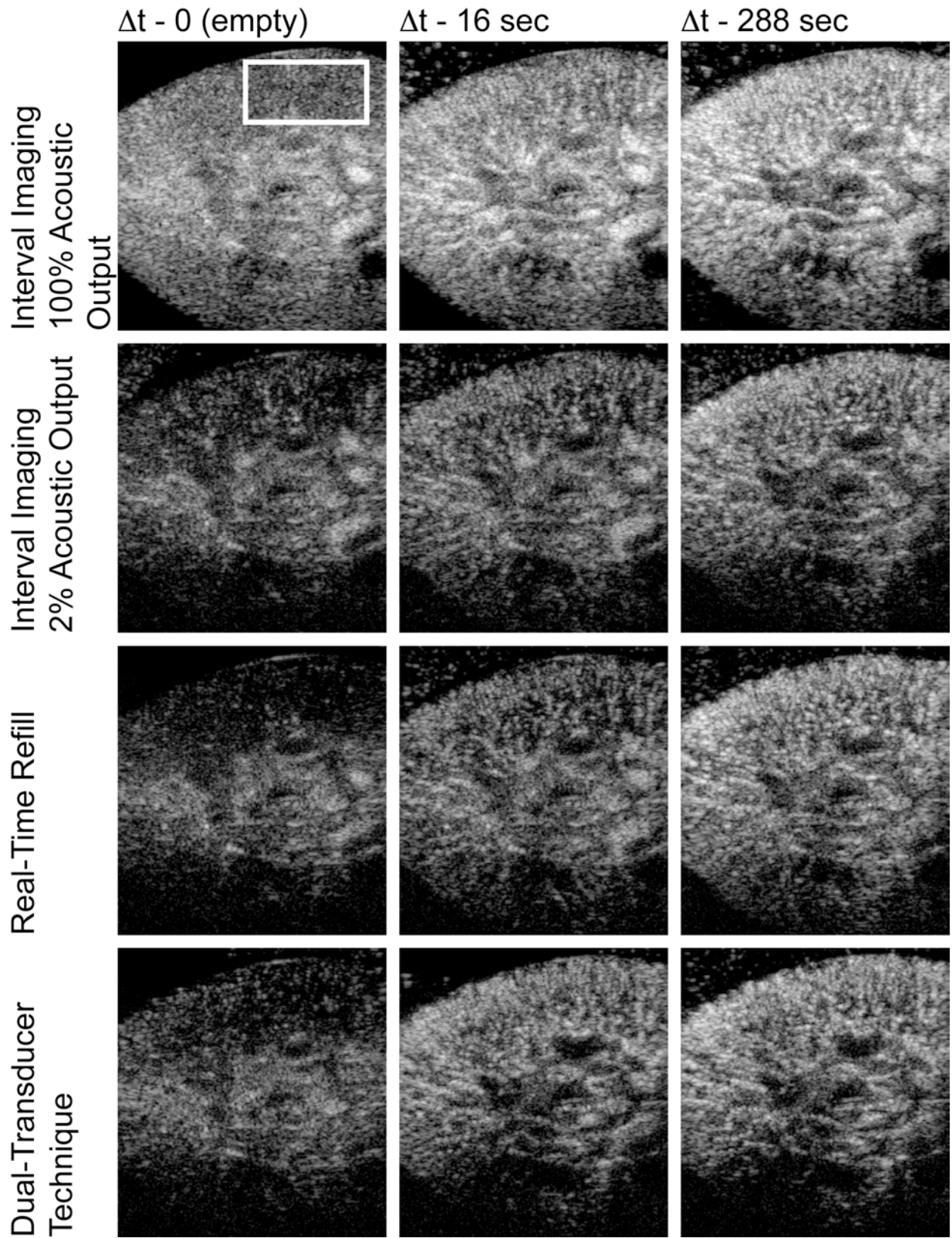


Fig. 3.

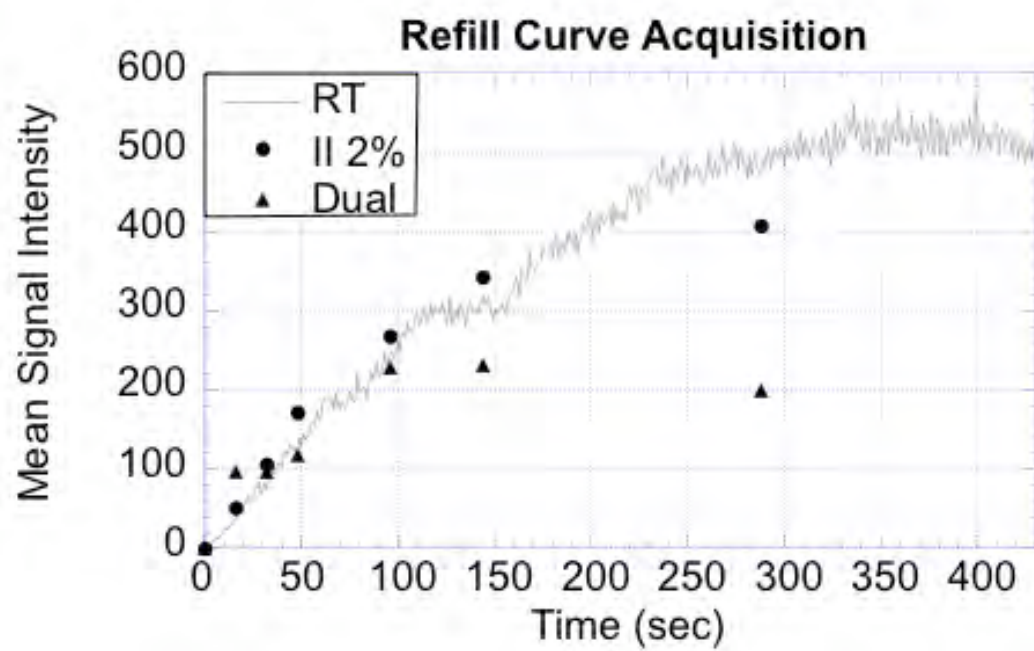


Fig. 4.

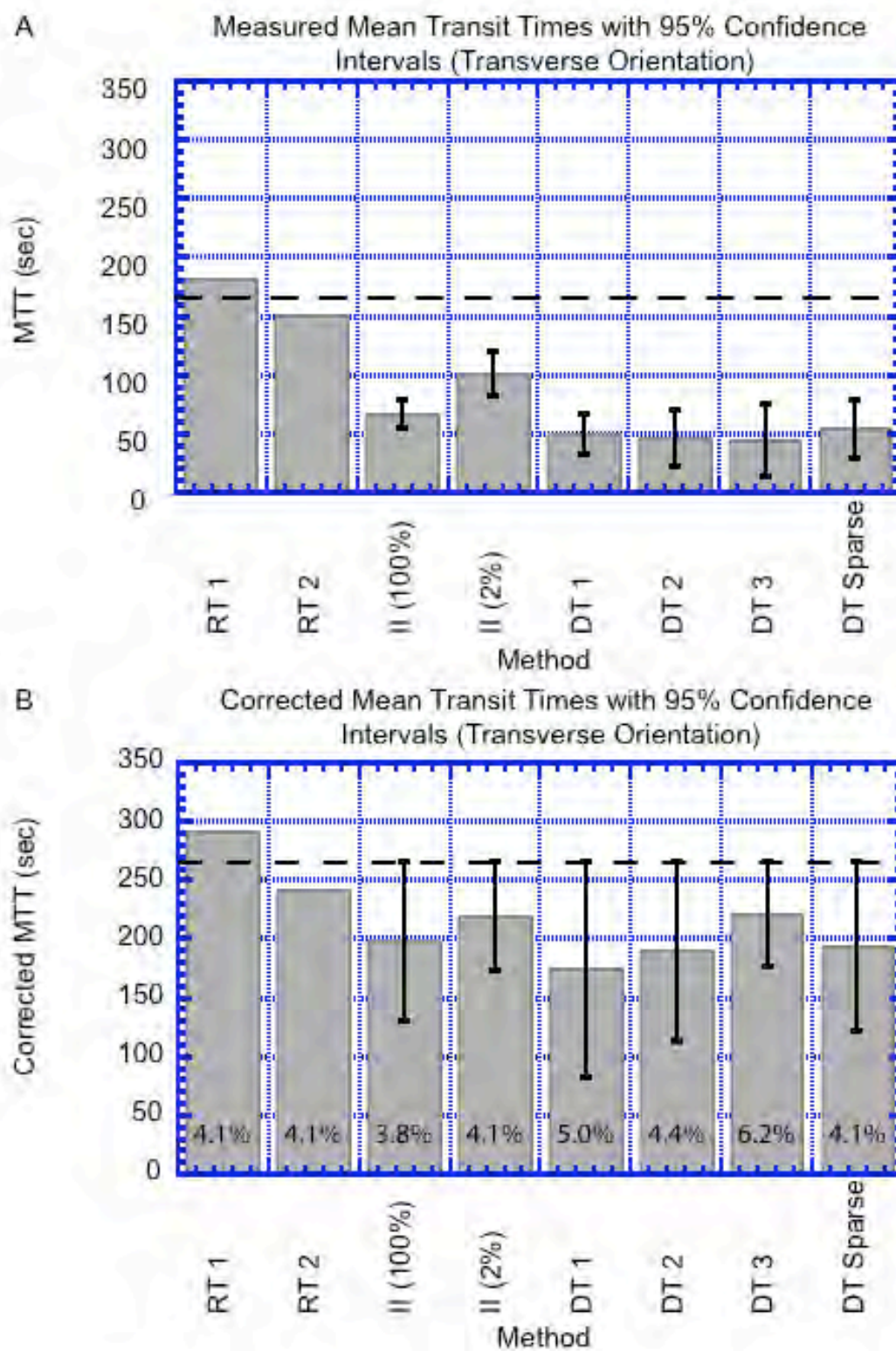


Fig. 5.

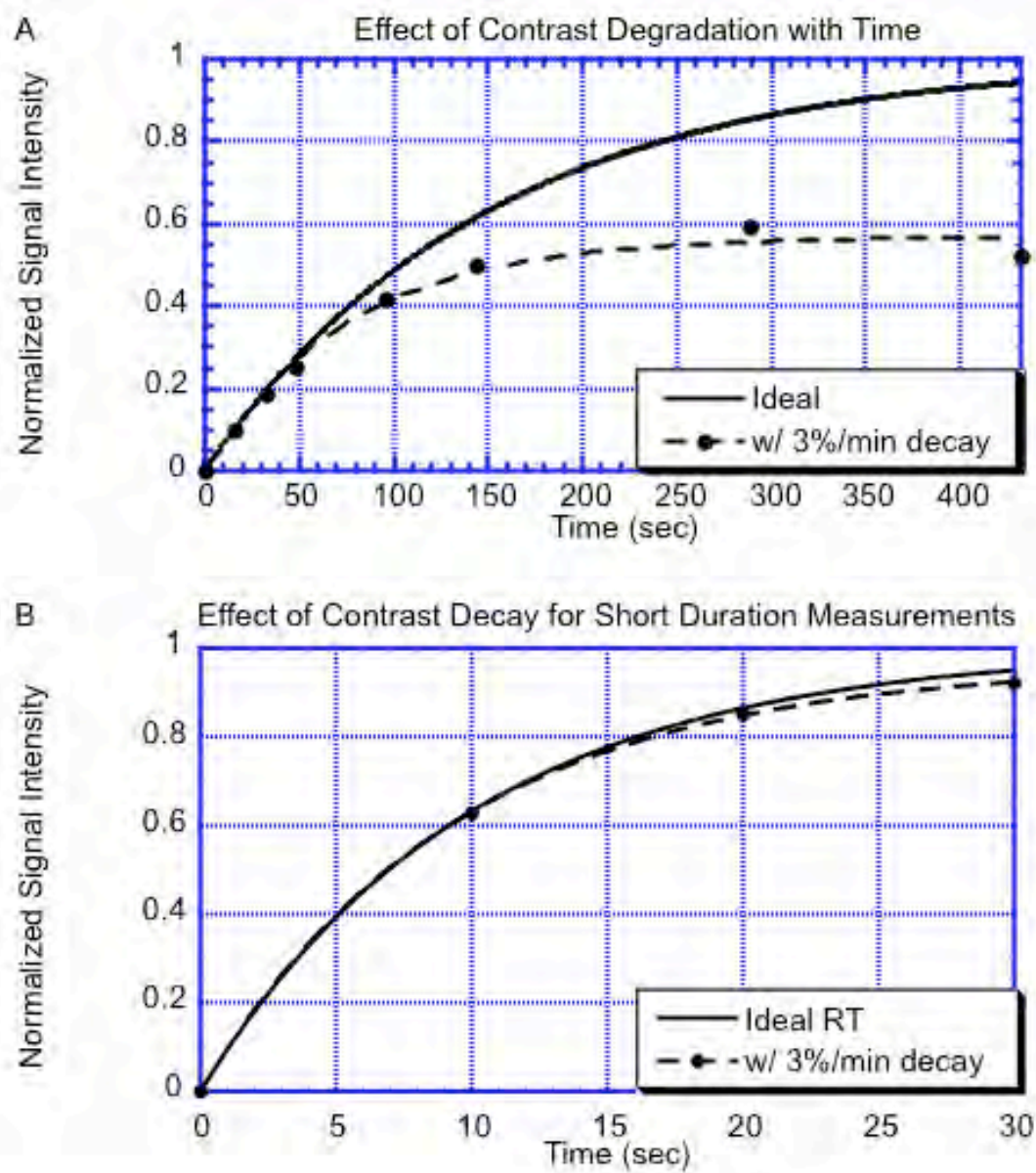


Fig. 6.

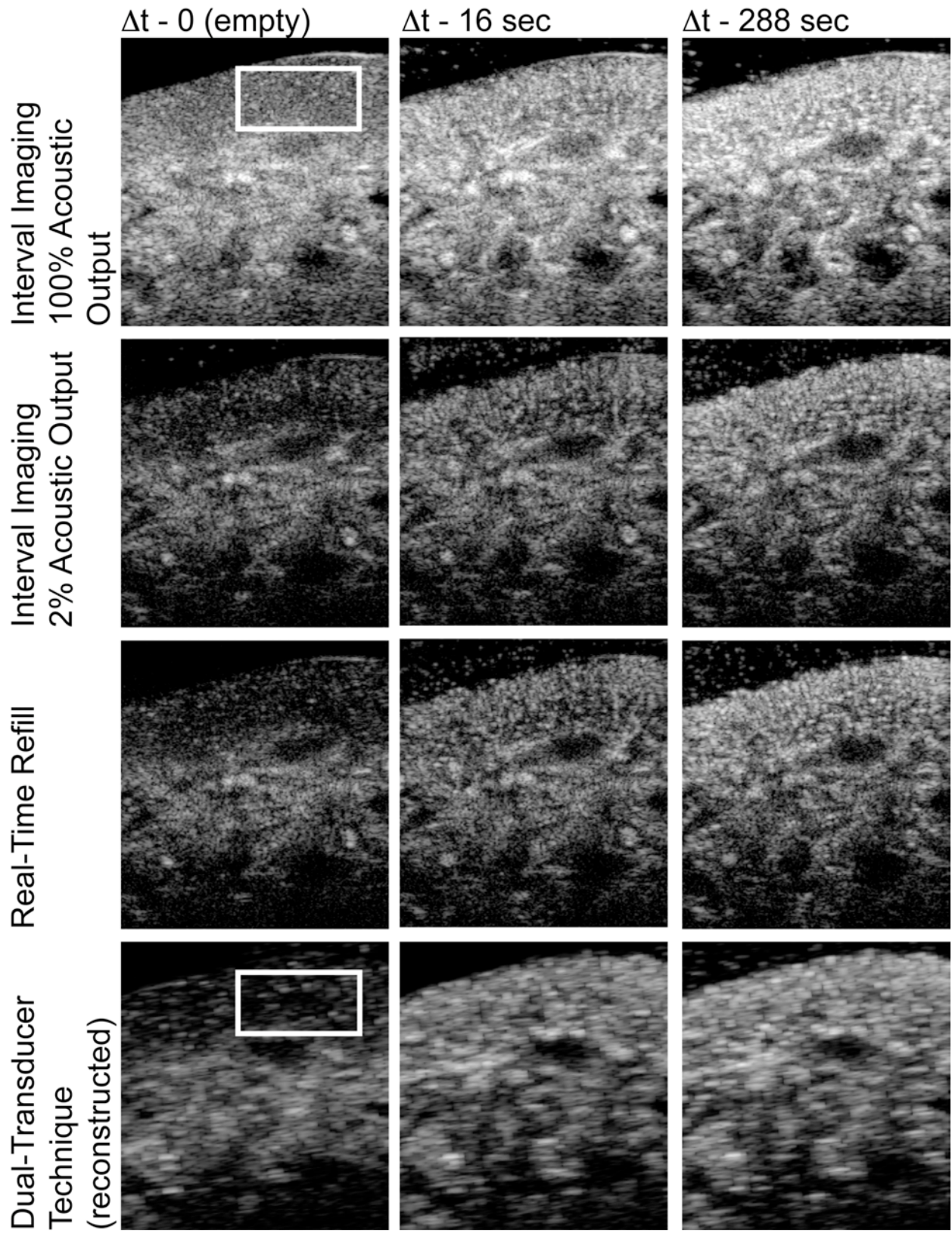


Fig. 7.

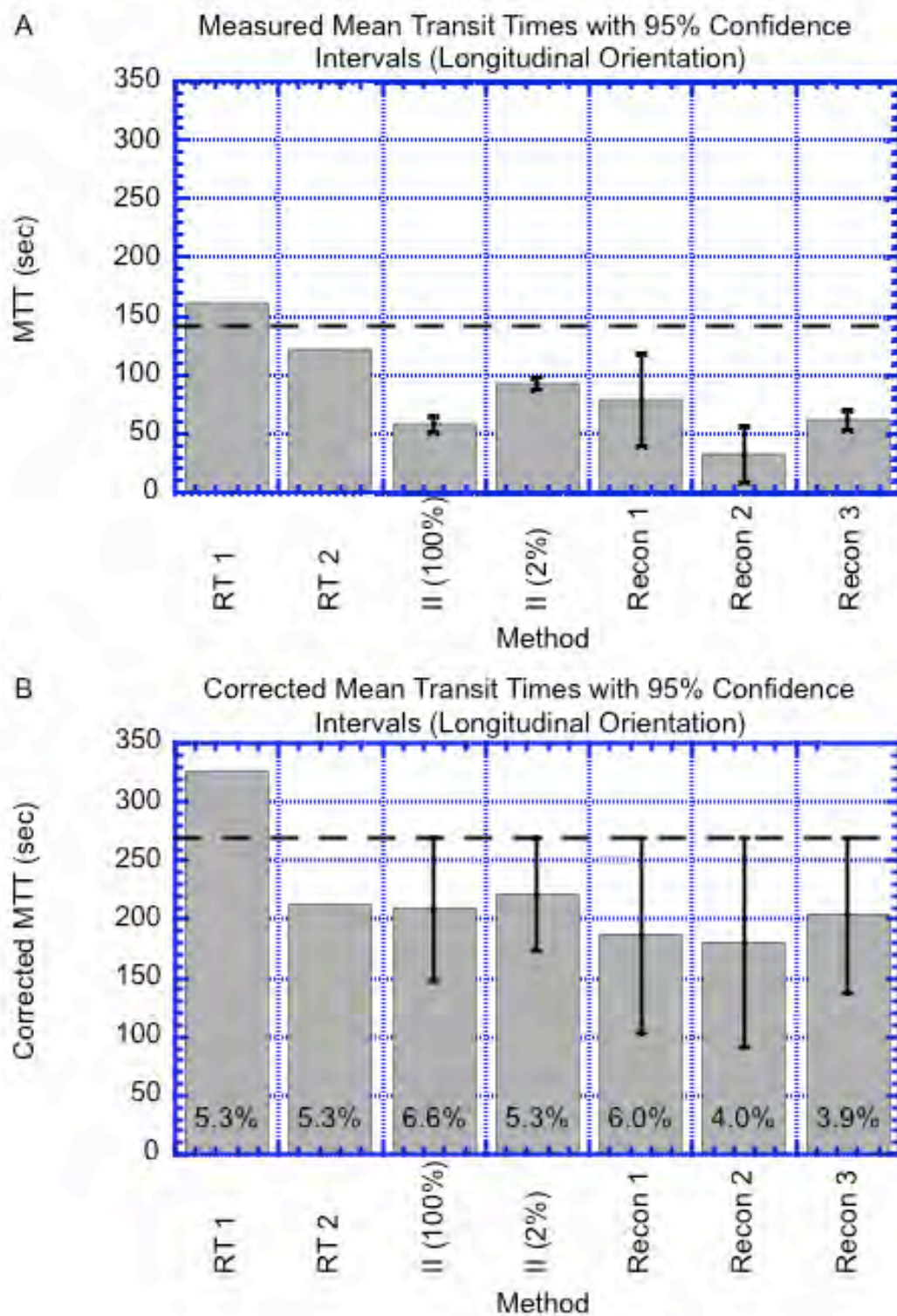


Fig. 8.

**PRELIMINARY RESULTS OF A NEW METHOD
OF 3D ULTRASOUND CONTRAST AGENT
MAPPING OF VASCULAR ANOMALIES FOR
CHARACTERIZATION OF BREAST MASSES**

**Gerald L. LeCarpentier, Nelson G. Chen,
J. Brian Fowlkes, and Paul L. Carson**

University of Michigan, Department of Radiology,
Ann Arbor, MI 48109

gllec@umich.edu

Doppler ultrasound and other imaging modalities have been used to assess characteristics of vasculature associated with malignant breast masses. Specific to our institution, promising results have been achieved in discriminating benign from malignant masses using Doppler vascularity measures in conjunction with ultrasound grayscale features. In addition to characterization, co-registration of sequential image volumes of malignant masses for sequential assessment chemotherapy treatment has been undertaken by our group.

The purpose of this work is to develop an innovative dual-transducer method to control the destruction and imaging of ultrasound contrast during 3D ultrasound scanning of suspicious breast masses. This method, which involves sequential scanning and co-registration of image volumes acquired during contrast refill, should provide mapping of vascularity around these masses and highlight the associated anatomic variation in mean transit time.

Progress of the construction and testing of the mechanical, electrical, and software components of the scanning apparatus are presented here. Eventually, this new imaging scheme will be evaluated in a small patient population to begin to establish the refill characteristics for a variety of suspicious breast masses, and appropriate mathematical models will be developed to characterize contrast agent refilling following destruction specific to the dual-transducer system. Experimental assessment of contrast agent life-span, destruction characteristics, and refill imaging has been undertaken in flow phantoms. The feasibility of producing accurate 3D refill maps will be evaluated, and a software system will be developed to visualize quantification of regional perfusion in and around the region of interest. Preliminary results are presented here.

The innovative technique currently in development may allow rapid 3D imaging of the refill rate and may also prove effective in imaging small slow-flow microvasculature. This may be particularly relevant in the detection of vascular anomalies associated with angiogenesis near new tumor growth, which in turn would likely improve the ability of ultrasound in discriminating benign from malignant breast masses as well as broaden existing knowledge of tumor physiology.

INNOVATIONS IN TECHNOLOGY

32476

Does real-time updating of volume-rendered three-dimensional ultrasound images significantly degrade target and device conspicuity compared to static three-dimensional ultrasound?

Rose SC, Nelson TR, Radiology, University of California, San Diego Medical Center, San Diego, CA*

Objective: The aim of this study was to determine whether activation of real-time updating (4D US) of volume-rendered (VR) 3D US causes degradation of target or device conspicuity compared to static VR 3D US. By perceiving motion, VR 4D US imaging may be more intuitive and allow interactive feedback during interventional procedures.

Methods: US phantoms were made using a petroleum gel. Cornstarch was used to vary the echotexture. Three phantoms were created with (1) no starch (hypoechoic), (2) 5 ml of starch (isoechoic), and (3) 15 ml of starch (hyperechoic) added. Each phantom had 2-cm diameter hypoechoic, isoechoic, and hyperechoic gel targets imbedded. Implanted devices were a 22-gauge needle and a 14-gauge radiofrequency ablation probe (shaft and tines) introduced into the background gel at 20 and 60 degree inclinations. Identical 3D US volume data sets were acquired with the static mode (3D US) and real-time updated mode (4D US). Combinations of 7 postprocessing display parameters were tested. Conspicuity of the targets and devices were judged on a five-point visibility scale. Ratings for 4D US were compared to 3D US for each tested variable.

Results: Conspicuity of the target lesions and devices varied widely, from perfect visualization to not identifiable, depending on background and target echotexture and which postprocessing parameters were used. Activation of 4D US resulted in no change, degradation, or improvement of conspicuity in 66.1%, 25.4%, and 8.5% of targets, respectively, and 80.3%, 14.8%, and 4.8% of devices, respectively, compared to static VR 3D US images.

Conclusions: 4D US VR does not result in significant reduction in target and device conspicuity compared to 3D US VR imaging, and may be feasible for interventional applications in an appropriate acoustic environment and with correct selection of postprocessing imaging parameters.

32824

A new dual-transducer method of three-dimensional ultrasound contrast agent imaging of vascularity

LeCarpentier GL, Chen NG, Fowlkes JB, Carson PL, Radiology, University of Michigan, Ann Arbor, MI*

Objective: Although promising results have been achieved in assessing benign from malignant masses in the breast, prostate, and other organs using Doppler ultrasound, certain limitations remain. Of particular interest is slow flow and small vessel imaging in 3D. The purpose of this work is to develop a dual-transducer (DT) method of controlling the destruction and imaging of ultrasound contrast in 3D, aimed specifically at imaging vascular anomalies in these suspicious masses.

Methods: To date, all experimental procedures have been performed on flow phantoms. As controls, contrast (definity) flows at various speeds and concentration were imaged laterally in a tube phantom using a GE Logic 9 in a contrast imaging mode (GE9). In the DT scenario, cross-sectional images were acquired along the tube, and sequential scanning of image volumes acquired during contrast refill was performed. A Toshiba Power Vision 8000 (TPV) was used to destructively sweep the region and create a contrast-cleared front in the volume. The GE9 transducer followed behind that of the TPV and imaged continuously. The transducers were set various distances apart

while both swept the region on a mounted and controlled motor system. The sweep speed was held constant such that the distances between the destruction and imaging transducers would correspond to particular times during refill. Sequential image volumes were reconstructed from the GE9 data sets.

Results: Contrast agent concentrations less than 4:10000 were linearly related to signal intensity in a 6-mm tube. In the control sets, the expected 2D parabolic evolution of the flow profile was seen. The DT images did not suffer the 2D limitation, and image planes reconstructed as slices along the tube displayed striking clarity and clear definition of flow profile information.

Conclusions: Preliminary results suggest that slow flow can be visualized and tracked in 3D, and the DT technique may provide measures of tissue refill characteristics unobtainable with current Doppler methods. Given the correlation of neo-vascularization and tumor growth, this imaging method has the potential of detecting and enhancing understanding of changes in microvasculature at early stages of tumor development.

32368

Precise real-time superposition of ultrasound with reformatted CT-MR-SPECT-PET images using three-dimensional navigation

*Bale RJ,*¹ Kovacs P,¹ Lang B,¹ Knoflach M,¹ Bodner G,¹ Profanter C,² Prommegger R,² Jaschke W,¹ 1. Radiology I (SIPLab), University Hospital Innsbruck, Innsbruck, Austria, and 2. Surgery, University Clinic Innsbruck, Innsbruck, Austria*

Objective: The aim of this study was to present a novel technique of multimodal imagefusion using 3D navigation.

Methods: The patient is immobilized, and the CT/MR/SPECT/PET images are sent to the StealthStation navigation system. After registration of the patient, the ultrasound probe is calibrated. The navigation system tracks the position of the ultrasound probe and calculates the probe in relation to the patient's anatomy. The preoperative CT/MR/SPECT/PET images are reformatted to the orientation of the ultrasound image and display next to the ultrasound image. Images can be taken as snapshots or acquired in brief movies. Being able to display the corresponding modalities side-by-side helps the radiologist to interpret the anatomy shown in the oblique ultrasound planes. Special software tools allow for blending the correlated CT/MR/SPECT/PET and ultrasound images. Color Doppler ultrasound may be used for more detailed vascular information.

Results: SonoNav allows for precise real-time correlation of CT/MR/SPECT/PET with ultrasound images in variable reformatted planes. However, the accuracy has to be evaluated in further studies.

Conclusions: The resulting information is very helpful for anatomic studies as well as for conclusive multimodality-based diagnosis.

31067

Ultrasound goes to the digital movies: Cine-loops and PACS software

Kovacs P, Peer S, Gruber H, Jaschke WR, Bodner G, Radiodiagnostics I, University Hospital, Innsbruck, Tyrol, Austria*

Objective: Ultrasound is inherently dynamic and allows for functional evaluation of various organ systems. Normally, this information is only available to the examiner, and demonstration is impossible except with videotaping. Our aim was to bring back in mind that ultrasound can be presented in a dynamic way using latest PACS (picture archiving and communication system) software.

Methods: On an HDI-5000 (ATL, USA), cine-loop software allows picture-by-picture transfer of dynamic investigations to PACS systems. Tools in the J-Vision PACS software (TIANI, Austria) play these pictures in a movie sequence and provide dynamic informations to all

877. P4.125. Assessment Of A 3D Dual-Transducer Ultrasound Contrast Agent Technique For Vascular Imaging

N.G. CHEN, J.B. FOWLKES, P.L. CARSON AND G.L. LECARPENTIER

University of Michigan, Ann Arbor, MI

3D ultrasound imaging of vascular flow and possible anomalies requires contrast refill images for all slices. Impracticably long scan times are needed for 3D real-time (RT) imaging. We assessed a modified contrast interruption dual-transducer technique (DTT) in overcoming this limitation. A positioning system was designed to control separation distance (SD) and to translate in-line two transducers (one to clear, one to image) above a slow-flow phantom consisting of a foam encased thin-walled tube. By performing multiple sweeps using various SD, image volumes at various times during refill were obtained. Lateral images extracted from reconstructed 3D DT volumes were compared with theoretical flow profiles. Preliminary measurements of a perfused kidney phantom were also compared to RT imaging. For both flow rates measured, contrast imaged in the tube approximated predicted profiles with slight tip truncation where excessive contrast destruction was the most likely. Regardless, flow velocities computed using measured profiles were within 15% of their predicted value on average. DTT scans required ~21-28 sec, 80-140 times less than corresponding RT scans. 3D DT scans of the kidney showed remarkable detail, and lateral images extracted from the reconstructed volume were consistent with measured RT. Conclusion: By drastically reducing scan time, the DTT makes reproducible 3D contrast-interruption scanning feasible and may facilitate 3D visualization of slow flow and microvascular refill.

Acknowledgment: This work was sponsored by federal grants DAMD170110327 and R01DK56658.

RSNA2005

Connecting for Lifelong Learning



November 27-December 2
McCormick Place- Chicago

Home

- ▶ Meeting Program
- ▶ Technical Exhibition
- Image Interp. Session
- ▶ Downloads
- Career Connection
- Attendance 2005
- Past Meetings
- Future Meetings
- RSNA.org
- Contact Us



Virtual Briefcase | Search | Email this Event | Login

RSNA 2005 > [A 3D Dual-Transducer Ultrasound Technique for the ...](#)

Scientific Papers

CODE: SSE06-05

SESSION: Ultrasound (Vascular)

A 3D Dual-Transducer
Ultrasound Technique for the
Assessment of Vascular Flow
Using Contrast Agent Imaging

TOOLS



Briefcase [Add to Briefcase](#)
[Print](#)
[Email](#)
[Event](#)

PARTICIPANTS

Presenter

Nelson [Chen](#) MS ★

Abstract Co-Author

Jeffrey [Fowlkes](#) PhD ★

Paul [Carson](#) PhD ★

Gerald [LeCarpentier](#) PhD ★

★ - Author stated no financial disclosure

▲ - Disclosure information unavailable

DATE: [Monday, November 28 2005](#)

START TIME: 03:40 PM

END TIME: 03:50 PM

LOCATION: [E353A](#)

PURPOSE

Imaging slow vascular refill in 3D using ultrasound contrast requires images be acquired during the entire refill time for each slice in the volume. Thus, 3D real-time imaging (RT) and interval-imaging (I-I) techniques are extremely time-intensive. Our purpose was to assess a dual-transducer technique (DT) to overcome this problem.

METHOD AND MATERIALS

A computerized positioning system was developed to control separation distance and translation of two transducers (one to clear contrast, one to image) mounted inline. A perfused porcine kidney was used as the experimental flow phantom. By varying separation distance and performing multiple sweeps, the imaging transducer captures a series of images in time and space that are constructed into a 4D contrast refill volume. Contrast mean transit times (MTTs) were calculated for select ROIs in sample transverse and longitudinal image planes extracted from 3 reconstructed DT volumes. These were compared with MTTs acquired in similar planes using RT and I-I. Because of systemic contrast decay in this slow-flow model, contrast intensities observed during successive RT measurements were used to estimate decay rates and correction factors for comparisons of RT, DT, and I-I MTTs.

RESULTS

DT produced image volumes of remarkable spatial detail at scan times 4% of that needed for RT acquisition, and 1.6% of that needed for I-I. MTTs for transverse DT images were consistent with each other though slightly shorter than those of corresponding I-I and RT scans. Accounting for contrast decay over time, all MTTs were consistent within statistical significance ($p < 0.05$). Longitudinal DT images extracted from the 3D volumes correlated similarly with measured longitudinal RT and I-I image sequences.

CONCLUSION

The DT technique offers a means to acquire 3D US contrast image volumes where conventional schemes would be unrealistic. It provides reproducible vascular refill information, and estimated MTTs are consistent with current methods after accounting for contrast decay, which may be minimal in vivo. Results suggest the technique may facilitate 3D visualization of slow flow and microvascular refill. This work was sponsored by federal grants DAMD170110327 and R01DK56658.

- 201709 A Comparison Between Acoustic Output Indices in 2D and 3D Ultrasound in Obstetrics**
Sheiner E, Strassner HT, Hussey MJ, Pombar X, Abramowicz JS Obstetrics and Gynecology, Rush University Medical Center, Chicago, IL*

OBJECTIVE: Three-dimensional (3D) ultrasound plays an important role in imaging of the fetus and is gaining popularity in prenatal diagnosis. While there are no studies regarding the safety of this novel technique, the short acquisition time and the post processing analysis are thought to decrease exposure and thus possible unknown effects of the ultrasound waves on the fetus. However, it is very difficult to evaluate the additional scanning time needed to choose an adequate scanning plane and to acquire a diagnostic 3D volume. The present study was aimed at comparing the acoustic output, as expressed by thermal index (TI) and mechanical index (MI), of conventional 2D and 3D volume acquisition during the third trimester of pregnancy.

METHODS: A prospective, observational study was conducted, using commercially available equipment (iU22, Philips Medical Systems). Third-trimester patients were randomly recruited from those scheduled for follow-up exams in order to complete a fetal anatomy survey. Sonographers were unaware of the data being sought. Data were collected regarding duration of the exam and specific time duration spent at each MI and TI during 2D and 3D ultrasound exams. Statistical significance was calculated using the Student *t* test for differences in continuous variables.

RESULTS: A total of 14 third-trimester ultrasound examinations were evaluated. Mean duration of the exam was 16.4 ± 3.5 minutes. Mean MI during the 3D volume acquisitions was significantly lower than the 2D B-mode ultrasound studies (0.73 ± 0.18 vs 1.11 ± 0.11 ; $P < .001$). Likewise, mean TI during the 3D examinations was significantly lower than the TI during the B-mode scanning (0.20 ± 0.08 vs 0.29 ± 0.11 ; $P = .004$). The 3D volume acquisitions added 1.41 ± 0.3 minutes of actual ultrasound scanning (not including data processing and manipulation or 3D display, which are all post processing steps).

CONCLUSIONS: Acoustic exposure levels during 3D ultrasound examination, as expressed by TI and MI, are lower than the 2D B-mode ultrasound. Therefore, as assessed by the output display indices, third-trimester 3D appears to be safe for the fetus.

- 202606 Accurate Tracking of Changes in 3D Doppler and Gray Scale Ultrasound as a Function of Time, Compression, and Scan Orientation**
*LeCarpentier GL,*¹ Zabuwala S,² Kapur A,⁴ Fowlkes JB,¹ Narayanasamy G,³ Carson PL¹*
 1. Radiology, University of Michigan, Ann Arbor, MI 2. Electrical Engineering, University of Michigan, Ann Arbor, MI 3. Applied Physics, University of Michigan, Ann Arbor, MI and 4. General Electric Global Research, Niskayuna, NY

OBJECTIVE: Detection of vascular anomalies and changes in volume and vascular characteristics of breast

masses may aid in their characterization or assessment of response to chemotherapy. The objective of this work is to determine our ability to (1) quantify local changes in blood volume using a 3D ultrasound (US) device under development and (2) accurately coregister breast image volumes acquired under different scan conditions.

METHODS: Five subjects (sb) participated in this preliminary study. Their breasts were positioned beneath a mammographic compression paddle modified to facilitate automated 3D US scanning with a GE Logiq 9. Image volumes (3 gray scale [GS] and 13 cardiac-gated color Doppler [CD]) were collected via computer interface at different times (4 sb), compression levels (4 sb), and/or orientation (1 sb). Using GS information alone, in-house image-based registration software (MIAMIFuse) was used to coregister image volumes under different conditions, and both hand-selected and Doppler-indicated fiducial points served as markers for registration accuracy. A scheme was also developed to automatically measure changes in blood volume (Δ BVs) for coregistered sequential CD scans.

RESULTS: Mean registration errors throughout the volumes were 0.5 mm for patients scanned at different times (interscan mean pixel displacement MPD = 9 mm), 1.1 mm for those scanned at multiple compressions (MPD = 3 mm), and 0.6 mm when image volumes were acquired at 2 transducer orientations. For CD cases, for a mean decrease in paddle distance (PD) of 7%, mean Δ BV increased by 18% for 2 cases and decreased for 4 by 30%. For mean PD decrease of 15%, Δ BV dropped 45%. Color pixel overlap for coregistered CD scans was >80%.

CONCLUSIONS: Despite variation in patient positioning as shown by MPD, sequential GS and Doppler scans can be accurately coregistered for quantitative evaluation of changes in mass volumes and blood flow. Results suggest that changes in blood volume can be detected as a result of compression variation, and these detected changes may aid in detecting vascular anomalies associated with malignant breast masses. This work was supported by NIH Grants P01 CA87634 and R01 CA91713.

- 202446 A 3D Dual-Transducer Ultrasound Technique for the Assessment of Vascular Flow Using Contrast Agent Imaging**
*Chen NG,*¹ Fowlkes JB,^{2,1} Carson PL,^{2,1} LeCarpentier GL²*
 1. Biomedical Engineering, University of Michigan, Ann Arbor, MI and 2. Radiology, University of Michigan, Ann Arbor, MI

OBJECTIVE: Imaging slow vascular refill in 3D using ultrasound contrast requires images be acquired during the entire refill time for each slice in the volume. Thus, 3D real-time imaging (RT) and interval-imaging (I-I) techniques are extremely time intensive. Our purpose was to assess a dual-transducer (DT) technique to overcome this problem.

METHODS: A computerized positioning system was developed to control separation distance and translation of 2 transducers (1 to clear contrast, 1 to image) mounted inline. A perfused porcine kidney was used as the experi-

mental flow phantom. By varying separation distance and performing multiple sweeps, the imaging transducer captures a series of images in time and space that are constructed into a 4D contrast refill volume. Contrast mean transit times (MTTs) were calculated for select ROIs in sample transverse and longitudinal image planes extracted from 3 reconstructed DT volumes. These were compared with MTTs acquired in similar planes using RT and I-I. Because of systemic contrast decay in this slow-flow model, contrast intensities observed during successive RT measurements were used to estimate decay rates and correction factors for comparisons of RT, DT, and I-I MTTs.

RESULTS: DT produced image volumes of remarkable spatial detail at scan times 4% of that needed for RT acquisition and 1.6% of that needed for I-I. MTTs for transverse DT images were consistent with each other though slightly shorter than those of corresponding I-I and RT scans. Accounting for contrast decay over time, all MTTs were consistent within statistical significance ($P < .05$). Longitudinal DT images extracted from the 3D volumes correlated similarly with measured longitudinal RT and I-I image sequences.

CONCLUSIONS: The DT technique offers a means to acquire 3D US contrast image volumes where conventional schemes would be unrealistic. It provides reproducible vascular refill information, and estimated MTTs are consistent with current methods after accounting for contrast decay, which may be minimal in vivo. Results suggest the technique may facilitate 3D visualization of slow flow and microvascular refill. (This work was sponsored by federal grants DAMD170110327 and R01DK56658.)

195962 Fetal Lung Volume Measured With 3D Ultrasonography in Pregnancies at Risk for Pulmonary Hypoplasia

Gerards F,^{*1} Twisk JW,² van Vugt JM¹

1. Obstetrics and Gynecology, VU University Medical Center, Amsterdam, Netherlands and
2. Biostatistics, VU University Medical Center, Amsterdam, Netherlands

OBJECTIVE: Pulmonary hypoplasia is mostly secondary to congenital disorders or complications during pregnancy, causing thoracic compression, inhibition of fetal breathing movements, or a net loss of lung fluid. The purpose of this study was to determine whether lung volume measurements with 3D ultrasonography could predict the occurrence of pulmonary hypoplasia in complicated pregnancies.

METHODS: In this prospective study, 1 to 4 scans of the fetal lung were obtained in 51 pregnancies complicated by various disorders or complications with regard to pulmonary hypoplasia. Using the freehand with positioning method, 2 to 5 volumes of the entire chest were acquired. Each lung was manually traced in the transverse plane from the fetal clavicles to the dome of the diaphragm and (re-) measured 3 times by the same examiner. From these 2D outlines the built-in program of the ultrasound machine automatically constructed a 3D model of the lung. The lung volume measurements were compared with the longitudinal reference intervals of fetal lung volumes for each gestational age obtained from uncomplicated pregnancies.

RESULTS: Of the 51 infants, 14 (27.5%) had pulmonary hypoplasia on postmortem examination, and in 8 (15.7%) infants, pulmonary hypoplasia was suspected because of the clinical and radiologic presentation. When combining oligohydramnios caused by premature rupture of membranes, the renal and urinary tract anomalies, the skeletal and neuromuscular malformation, and other disorders, the overall sensitivity was 86% (confidence interval [CI] $\pm 15\%$), the specificity 100%, positive predictive value (PPV) 100%, and negative predictive value (NPV) 88% (CI $\pm 12.7\%$) in predicting pulmonary hypoplasia. When comparing the lung volume measurements of the intrauterine growth-restricted fetuses caused by uteroplacental insufficiency with the normal curves based on estimated fetal weight, sensitivity, specificity, PPV, and NPV of 100% was achieved. The intraclass correlation coefficient was 0.99 for both lungs.

CONCLUSIONS: 3D lung volume measurements seem to be useful in predicting pulmonary hypoplasia prenatally.

201434 Improved 3D Ultrasound of Fetal Anatomy Using a Virtual Reality Rendition System

Brezinka C,^{*1} Groenenberg IA,¹ Koning AH,² Galjaard R,³ Steegers EA,¹ van der Spek PJ²

1. Division of Obstetrics/Perinatal Medicine, Erasmus MC, Rotterdam, Netherlands
2. Bioinformatics, Erasmus MC, Rotterdam, Netherlands and 3. Clinical Genetics, Erasmus MC, Rotterdam, Netherlands

OBJECTIVE: To create a hologram-like virtual 3D image of fetal ultrasound that can be manipulated by an operator.

METHODS: Images obtained from a GE Voluson 730 Expert system are transferred to the BARCO I-Space, a 4-walled virtual reality system. In the I-space, investigators are surrounded by computer-generated stereo images, which are projected on the walls and floor of a purpose-built room. Looking at the images wearing polarizing lens glasses, the viewer perceives depth, can walk around them, and can look at the images from below. We use a 3D texture mapping technique to render 3D visualizations of volumetric data sets.

RESULTS: Biocular depth perception provides a realistic 3D illusion that allows better assessment of fetal structures. Direct manipulation of the virtual 3D image by cutting it with a virtual pointer further augments the understanding of the spatial arrangement of fetal structures. By applying 1 or more clipping planes to the volume, it becomes possible to have an unobstructed view of any part of fetal anatomy.

CONCLUSIONS: Operators who are new at 3D ultrasound find it much easier to render the images they have obtained on their ultrasound machines after they have learned to move the image around and move around it themselves in the I-space. One of the great advantages of this method is that several observers, 1 of them usually an instructor, can stand around the hovering object and watch simultaneously while it is being worked upon with the joystick-pointer.

Print 

Submitted Abstract

on September 29, 07:23 PM

for 2007aium

Proof

CONTROL ID: 297009

CONTACT (NAME ONLY): Gerald LeCarpentier

PRESENTER: Gerald LeCarpentier

DATE/TIME LAST MODIFIED: September 29, 2006, 7:23 PM

Abstract Details

PRESENTATION TYPE: Scientific Paper (oral)

CATEGORY: Basic Science

SUB-CATEGORY: Contrast Agents (non-clinical)

AWARDS:

Abstract

TITLE: 3D Perfusion Measurements Using a Dual-Transducer Ultrasound Contrast Agent Technique

AUTHORS (LAST NAME, FIRST NAME): Chen, Nelson G²; Fowlkes, J. Brian^{1, 2}; Carson, Paul L^{1, 2}; LeCarpentier, Gerald L¹

INSTITUTIONS (ALL): 1. Radiology, University of Michigan, Ann Arbor, MI, USA.

2. Biomedical Engineering, University of Michigan, Ann Arbor, MI, USA.

ABSTRACT BODY:

OBJECTIVE : Perfusion mapping requires measures of mean transit time (MTT) as well as fractional blood volume (%BV). So called interval-imaging (I-I) methods may provide perfusion measures, but may be time prohibitive in 3D. Our purpose was to assess a previously reported dual-transducer technique (DT) extended to actual perfusion measurements, evaluated at 2 different flow rates.

METHODS: In-line separation distance and translation of two transducers were controlled by a computer interfaced positioning system. An imaging transducer captures a series of images at a given delay behind a clearance transducer such that multiple sweeps at varying transducer separations can be reconstructed into a 4D contrast refill volume. Such sweeps were performed over a fixed porcine kidney flow phantom perfused at 2 flow rates, and I-I scans were performed through a single plane, which was compared to a single plane extracted from the DT volume. Each test scenario was repeated at least 4 times. Signal levels throughout a region of interest (ROI) were normalized to the signal level in a major vessel to obtain %BV over time and at steady state, and contrast MTTs and overall perfusion rates were calculated for both methods.

RESULTS: For a volume the size of our kidney phantom, I-I in 3D would require 63 times as long an acquisition duration as that for the DT method. There were no statistically significant differences between perfusion estimates in the ROI using DT versus I-I. The trends in perfusion rate varied with flow rate as expected; however, local perfusion rates in the ROI did not closely follow overall input flow rates for either method. Perfusion rates were more dependent on %BV than MTT in all cases.

CONCLUSIONS: Consistency between DT and I-I suggests that DT is a viable alternative in

measuring perfusion and shows promise over I-I methods when 3D information is preferred. Since our normalization scheme is performed on each image, %BV estimates are independent of contrast decay over time. Strong dependence of perfusion calculation on %BV may indicate vessel dilation at higher flow rates, and a reproducible method for estimating %BV is essential. This work was sponsored by grants DAMD170110327, R01DK56658, and P01CA87634.

(No Table Selected)